

Techno-economic assessment of offshore wind energy potential at selected sites in the Gulf of Guinea

Olayinka S. Ohunakin^{a,b,*}, Olaniran J. Matthew^c, Muyiwa S. Adaramola^d, Opemipo E. Atiba^a, Damola S. Adelekan^a, Oluwadamilare O. Aluko^e, Emerald U. Henry^a, Victor U. Ezekiel^a

^a The Energy and Environment Research Group (TEERG), Mechanical Engineering Department, Covenant University, Ogun State, Nigeria

^b Faculty of Engineering & the Built Environment, University of Johannesburg, South Africa

^c Institute of Ecology and Environmental Studies, Obafemi Awolowo University, Ile-Ife, Osun State, Nigeria

^d Faculty of Environmental Sciences and Natural Resource Management, Norwegian University of Life Sciences, Ås, Norway

^e Gommyr Power Networks Limited, Scotland, United Kingdom

ARTICLE INFO

Keywords:

Offshore
Wind energy potential
Weibull
Levelized cost of energy
Gulf of Guinea

ABSTRACT

Offshore wind power has been found to stand out among the most dynamic renewable energy technologies. With its long coastal line, Nigeria has an overwhelming advantage in developing marine energy resources to relieve the power crisis effectively. This work analyzed and characterized observation data of sea-surface wind speed and direction at 30-minute intervals between 1979 and 2015 at five synoptic offshore stations in the Gulf of Guinea. The seasonal variations in hourly surface wind speed and directions as well as the Weibull distribution of wind speed and wind power at 100 m hub height were examined. The wind shears, capacity factors, and accumulated energy outputs for seven offshore wind turbine types were determined for the selected locations. In addition, the economic analysis of the selected offshore turbines using levelized cost of energy was carried out, while sensitivity analysis of the total levelized cost of energy to key input parameters was further determined. The results revealed large spatial and temporal variations in wind speed and wind power in the Gulf of Guinea. The most viable offshore site for wind energy exploitation was Agbami (the deepest offshore site), while Bonny (the shallow coastal site) had the least. The findings established very good fits (having mean bias (between -0.08 ms^{-1} and -2.44 ms^{-1}), percentage bias (between -0.47% and -13.98%), correlation coefficients (between 0.97 and 0.98), Chi-square (between 0.2 and 1.2), and root mean square error (between 1.2 ms^{-1} and 3.1 ms^{-1}) between Weibull distribution and the actual wind data. The wind turbines with the highest and the lowest wind power densities, capacity factors, and power outputs across the seasons and sites were V236-15.0 MW and Siemens SWT113, respectively. The levelized cost of energy was considered for the deep waters due to the moderately high-capacity factors. The highest values ranged between 101.48 and 137.12 USD/MWh at Sea Eagle with V236-15 MW and V117-4.2 MW, respectively, while the lowest ranged from 52.29 to 69.66 USD/MWh at Agbami with V236-15 MW and Siemens (SWT113), respectively. The exploitation of Nigeria's offshore wind resources could also be dedicated to producing renewable hydrogen and can serve to meet the country's ambitious targets set for carbon neutrality by 2060.

1. Introduction

A transition to nature-friendly solutions for energy supply is very essential for the world in its quest toward carbon neutrality by 2060. To reduce greenhouse gases (GHG), adopting renewables will be of immense assistance [1]. Wind power is a promising and fast-emerging renewable energy resource for power generation. It is the most advanced among renewable sources, with the highest technological

readiness level [1]. It has shown great potential in mitigating climate change and stimulating the global economy while boosting energy security [2]. Nigeria's Energy Transition Plan (ETP) unveiled in 2021 sets out a timeline and framework for the attainment of emissions reduction; within the scope of the ETP, about 65% of Nigeria's emissions are affected [3]. This ambitious target of ETP set to meet carbon neutrality by 2060, can easily be achieved by fully exploiting the country's vast offshore wind and marine energy resources.

Several wind power projects have been completed in Africa, while

* Corresponding author.

E-mail addresses: olayinka.ohunakin@covenantuniversity.edu.ng, ohunakin@gmail.com (O.S. Ohunakin).

Nomenclature		
Symbol		
A	Rotor Blade Swept Area (m^2)	V_c Cut-in Wind Speed (m/s)
c	Weibull Scale Parameter (m/s)	V_f Cut-off Wind Speed (m/s)
C_f	Capacity factor (%)	V_j Mean Wind Speed (m/s)
C_I	Total investment cost (USD)	V_r Rated Wind Speed (m/s)
C_o	Scale factor (m/s)	
C_{om}	Operation and Maintenance Cost for the First year	
$C_{\text{om(esc)}}$	Present Worth of the Annual cost throughout turbine life	
d	Number of days in the month considered	
E_o	Accumulated Annual Energy Output	
e_{om}	Escalation of Operation and Maintenance	
E_{WT}	Annual Energy Output of Wind Turbine (kWh)	
$f(V)$	Probability Density Function	
$F(V)$	Cumulative Probability Function	
h	Hub Height (m)	
h_o	Measurement Height (m)	
k_o	Shape Factor Dimensionless	
kWh	Kilowatt hour	
n	Life of Turbine	
P_{eR}	Rated Electrical Power of the Turbine	
$P(V)$	Wind Power (W)	
r	Discount Rate (%)	
ρ	Air density (kg/m^3)	
k	Weibull Shape Parameter	
V	Wind Speed at Required Height (m/s)	
V_o	Wind Speed at Measured Height (m/s)	

Abbreviation		
BIAS	Mean Bias	
CAGR	Compound Annual Growth Rate	
CCMP	Cross Calibrated Multi-Platform	
CRF	Capital Recovery Factor	
DJF	December to February	
ETP	Energy Transition Plan	
GoG	Gulf of Guinea	
GWEC	Global Wind Energy Council	
JJA	June to August	
LCOE	levelized Cost of Energy	
MAM	March to May	
MSH	Mean Wind Shear (m^{-1})	
msl	Mean Sea Level	
MW	Mega Watts	
NDC	Nationally Determined Contributions	
PBIAS	Percentage Bias	
RMSE	Root Mean Square Error	
SON	September to November	
SW	South-Westerly	
USD	US Dollars	
WAM	West Africa Monsoon	
WPD	Wind Power Density	

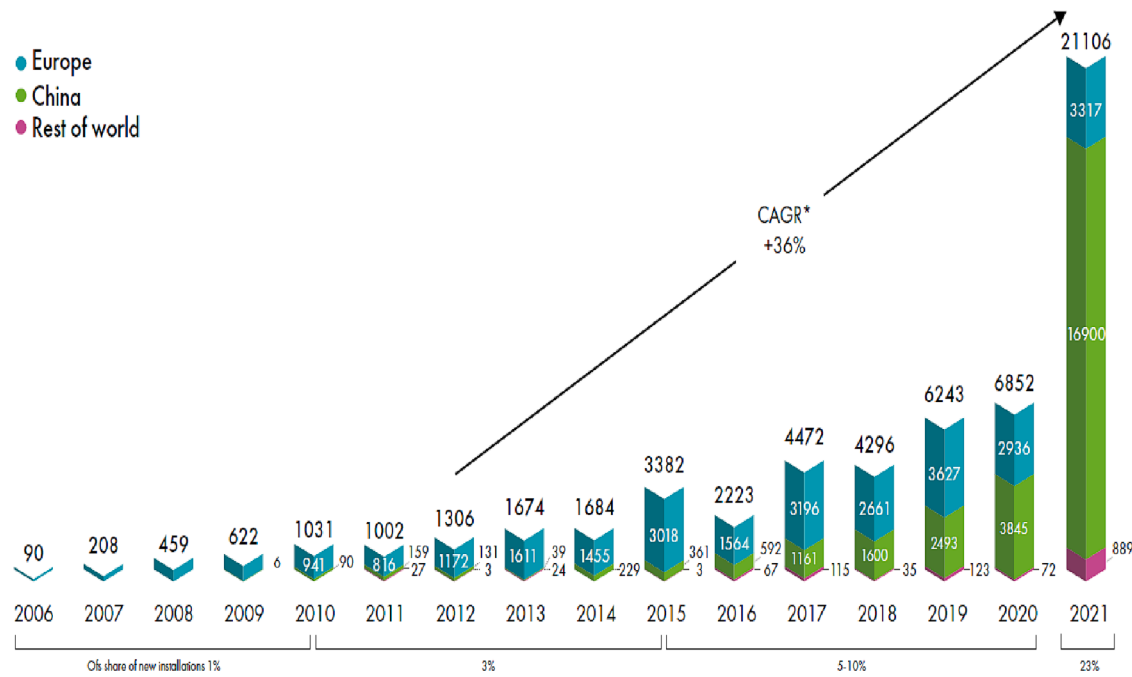


Fig. 1. New offshore installations 2006–2021 (MW). *Compound Annual Growth Rate. (Source: GWEC Market Intelligence, June 2022).

some are ongoing. However, wind power development in Africa is currently confined to onshore development due to inadequate knowledge of offshore wind potential across the continent [4]. Despite a long shoreline and the vast deposit of offshore wind resources, Africa is yet to exploit its offshore wind power. Offshore wind technology is rapidly growing worldwide, with an additional 21 GW installed globally in

2021, which makes it more than triple the capacity deployed in 2020 [5]. The total global offshore wind installed capacity as of 2021 rose to 50,623 MW from 257 operating projects [6]. This remarkable growth in offshore wind development is largely attributed to China, followed by the United Kingdom, Denmark, and the Netherlands in Europe and the rest of the world (Vietnam, Taiwan). The annual growth rate of the

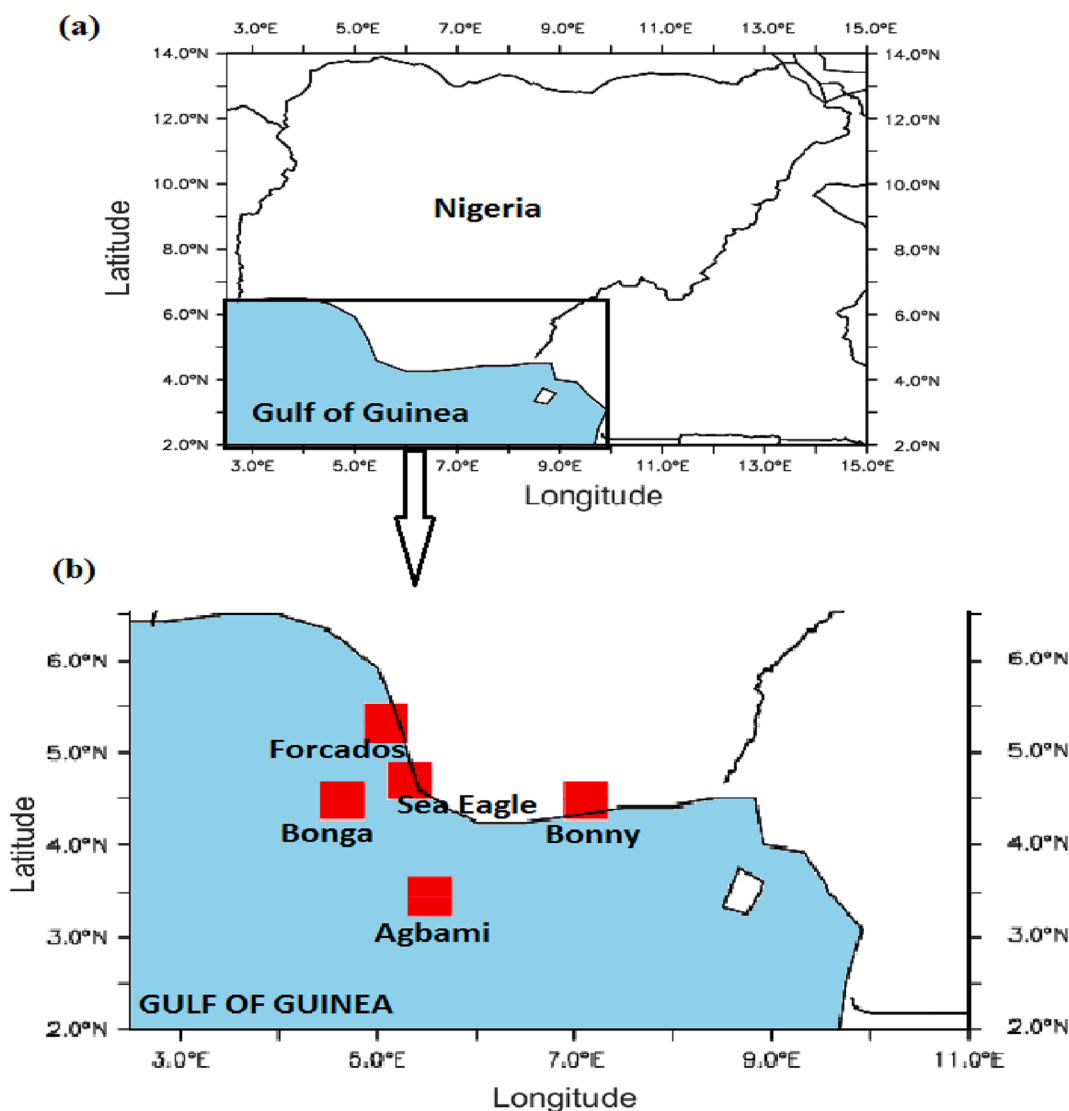


Fig. 2. Geographical locations of (a) the Gulf of Guinea within the Map of Nigeria and (b) offshore sea-surface wind observation stations selected for the study.

Table 1

Characteristics of the selected wind turbines.

Wind Turbine	Characteristics							
	Rated Power (MW)	Cut-in-Wind Speed (m/s)	Rated Wind Speed (m/s)	Cut-out-Wind Speed (m/s)	Hub Height (m)	Life (years)	USD/kW ¹	Turbine Cost (USD)
V164-9.5 MW ²	9.5	3.0	14.0	25	100	25	1200	11,400,000
V164-10.0 MW ³	10	3.0	14.0	25	100	25	1200	12,000,000
V117-4.2 MW ⁴	4.2	3.0	14.0	25	84	25	1214	5,100,000
V174-9.5 MW ⁵	9.5	3.0	14.0	25	110	25	1200	11,400,000
V236-15.0 MW ⁶	15	3.0	14.0	30	139	25	1200	18,000,000
GE (3.6sl) ⁷	3.6	3.5	14.0	27	100	25	1194	4,300,000
Siemens (SWT113) ⁸	3.2	2.5	13.5	22	80	25	1188	3,800,000

¹ (i) Authors approximated turbine specific cost from proprietary industry data, (ii) <https://www.irena.org/publications/2021/Jun/Renewable-Power-Costs-in-2020>. Accessed on February 06, 2023.

² <https://www.vestas.com/en/products/offshore/V164-9-5-MW>. Accessed on February 06, 2023.

³ <https://www.vestas.com/en/products/offshore/V164-10-0-MW>. Accessed on February 06, 2023.

⁴ <https://www.vestas.com/en/products/4-mw-platform/V117-4-2-MW>. Accessed on February 06, 2023.

⁵ <https://www.vestas.com/en/products/offshore/v174-9-5-mw->. Accessed on February 06, 2023.

⁶ <https://www.vestas.com/en/products/offshore/V236-15MW/V236-15MW#!technical-specifications>. Accessed on February 06, 2023.

⁷ http://www2.elo.utfsm.cl/~elo383/tareas/ge_36_brochure_new.pdf. Accessed on February 06, 2023.

⁸ https://www.thewindpower.net/turbine_en_887_siemens_swtt-3.2-113.php. Accessed on February 06, 2023.

Table 2

Sea-surface mean wind speed (hourly) characteristics at the offshore stations used in this study across the four astronomical seasons in the Gulf of Guinea.

Name of Offshore Site	Astronomical Season	Wind Speed Characteristics				
		Mean (ms ⁻¹)	Maximum (ms ⁻¹)	Standard Deviation (ms ⁻¹)	Coefficient of Variations (%)	Weibull Shape Factor k ₀
Forcados	DJF	3.77	9.00	1.44	38.20	2.84
	MAM	3.20	13.00	1.63	51.02	2.08
	JJA	2.77	9.00	1.56	56.42	1.86
	SON	2.89	10.00	1.79	62.00	1.68
Sea Eagle	DJF	4.92	14.36	1.68	34.14	3.21
	MAM	4.86	14.09	1.85	38.00	2.86
	JJA	6.13	13.84	1.95	31.82	3.47
	SON	6.04	12.22	1.78	29.46	3.77
Bonny	DJF	3.49	8.00	1.26	36.15	3.02
	MAM	2.56	9.00	1.39	54.31	1.94
	JJA	2.70	7.00	1.50	55.55	1.89
	SON	2.99	8.99	1.52	50.76	2.09
Bonga	DJF	5.90	10.50	2.02	34.29	3.20
	MAM	5.99	13.30	1.49	24.85	4.54
	JJA	4.59	10.55	1.52	33.11	3.32
	SON	4.49	12.44	2.02	45.10	2.37
Agbami	DJF	8.49	30.76	3.82	45.03	2.38
	MAM	12.78	22.69	3.41	26.70	4.20
	JJA	10.55	22.10	3.40	32.26	3.42
	SON	9.40	20.79	3.48	36.99	2.94

DJF = December - February.

MAM = March - May.

JJA = June - July.

SON = September - November.

offshore wind turbine is shown in Fig. 1. Despite the slow growth of offshore wind development when compared to onshore wind exploitation, offshore wind power still stood out among the most dynamic renewable energy technologies, based on installed capacity since 2010 [7], alongside its rapid technology developments, which showed potential for easier reduction of cost and the setting up of wind turbines in deep waters with the use of floating platforms [8]. Offshore wind power has also been found to trigger many benefits, such as job creation [9], enhancement of national energy security [10], global warming mitigation [11,12], etc. Inappropriate assessment of offshore wind resources, environmental impact assessment and transmission infrastructure [13], identification of appropriate turbine foundation technology, logistics, installation, operational stability, grid connectivity, and security [14] were found to be the major challenges hindering offshore wind power developments.

Nigeria ranks among the countries with very low per-capita power consumption globally, as opposed to around 15,000 kWh in developed nations [8]. In line with Nigeria's Nationally Determined Contributions (NDC), the country has shown keen interest in diversifying its energy mix by including renewable energy technologies (especially wind technology). This is done to accomplish a cumulative installed electric power capacity of about 20 % from renewables by 2030 (3.2 GW from wind, an additional 12 GW from large hydro, 3.5 GW from small hydro, and 6.5 GW of Solar PV) [15].

Wind energy resource has been highly underexploited in Nigeria; the only known is the installed 10 MW onshore wind farm in Katsina State, Nigeria. A number of studies have been conducted in assessing various onshore sites' potentials across the country; for instance, wind energy potential for small communities in South-South, Nigeria [16], wind potential over selected coastal cities in Nigeria [17], wind energy potential in selected sites from three geopolitical zones in Nigeria [18], economic analysis of wind energy conversion systems in Nigeria [19], wind energy potential and the economics of wind power generation in Jos, Plateau State, Nigeria [20], wind resources in North-East geopolitical zone, Nigeria [21], wind energy resources for electricity generation in North-Central region, Nigeria [22], wind energy evaluation for electricity generation in seven selected locations in Nigeria [23], wind

resource evaluation in six selected high-altitude locations in Nigeria [24], performance evaluation of wind turbines for energy generation in Niger Delta, Nigeria [25], and techno-economic evaluation of wind energy in South-West Nigeria [26]. However, for the offshore resource potential of Nigeria, very limited studies have been conducted to date, as given in Olaofe [27] and [28].

Recent studies have shown a significant reduction in offshore wind energy's levelized cost of energy (LCOE) and found it to be highly attributed to the reduced cost associated with technological innovation [29]. With about 800 km of coastal line, Nigeria has an overwhelming advantage in developing marine energy resources. Hence, research on marine energy resources in Nigeria, such as offshore wind energy exploitation and other marine renewable energy conversion systems, must be conducted. In Olaofe [27], an assessment of the offshore wind speed distributions at 10 m height was carried out over the South-West coast of Nigeria using a 6-hourly (00:00, 06:00, 12:00, and 18:00 UTC) Cross Calibrated Multi-Platform (CCMP) L3.0 over 10-years (2002–2011). In addition, the author (Olaofe [27]) further extended the work to consider an evaluation of the offshore wind resource over the coast of Africa [28], using CCMP L3.0 surface wind at 10 m height from 2001 to 2011. These works by Olaofe [27] and [28] were found to utilize 10-year generated satellite wind speed datasets to provide an overview only of the offshore wind energy resource distributions across the coasts of Nigeria (in the South-West) and Africa, respectively.

Despite the technological advancement in wind energy exploitations, comprehensive study regarding the assessment of wind potential is critical and essential in the earlier stages of the wind power project [30], alongside the variability of power [31], seasonality [32], the trend in wind power [33], economic aspects [34], and the effects on local climate [35]. In Icheni et al. [36], the stability state or condition of the atmosphere modifies the wind shear coefficient and energy generation from standard wind turbines. Hence, wind shear must be described most accurately because it is a major cause of cyclic loads of wind turbines [37]. In the coastal region, factors affecting wind speeds besides topography include the coastline orientation, water depth, air-sea temperature differences, prevailing wind speed and direction, latitude (related to the magnitude of solar radiative forcing), distance from the

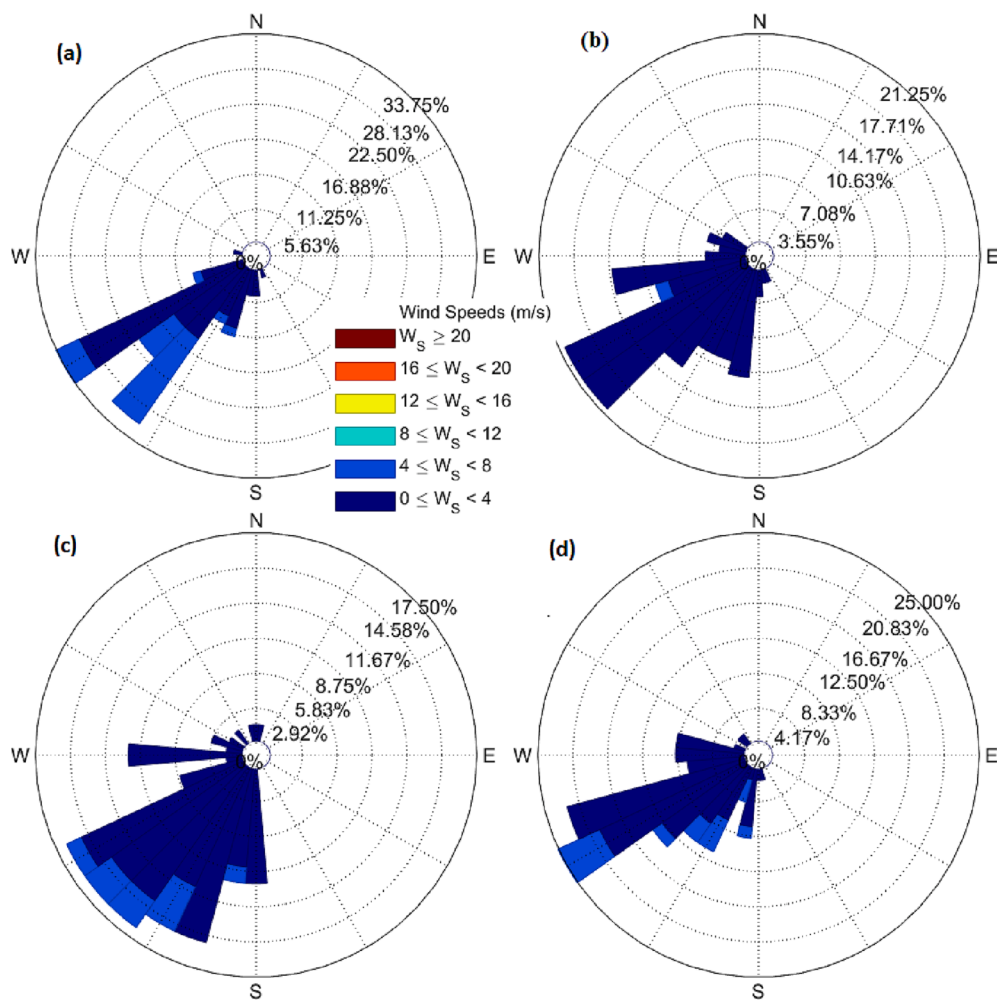


Fig. 3. Seasonal variations in wind rose compass distribution of sea-surface wind speed at the shallowest offshore observation station (Bonny) during the study period: (a) December to February, DJF; (b) March to May, MAM; (c) June to July, JJA; and (d) September to November, SON seasons.

coastal discontinuity, and fetch (i.e., the surface type over which the wind blows) [37]. These physical processes and determinants are important to carry out an extensive estimation of wind resources for wind energy applications. The variability of wind power is determined by wind behaviour at different timeframes, thus calling for special consideration of this perspective. The feasibility of a wind power project is greatly dependent on the inherent temporal characteristics of the wind, hence the need to quantify the temporal variability of the resource through variability indices at different timescales [38], resource versatility, and persistence [39]. The wind fluctuates in nature, resulting in an inconsistent power supply by a degree that is highly related to the location. Spatial comparisons of variability metrics will provide insight into the locations where wind energy is less intermittent and more dependable.

An in-depth analysis using reliable/sea-surface measured offshore wind data (found to be better and much more reliable than generated/satellite data) is thus essential to convert offshore wind potential into a real offshore wind farm. Hence, the aim of this present study is to conduct a comprehensive techno-economic assessment of offshore wind potential in the Southern Atlantic Ocean bordering the coastline of Nigeria (also known as the Gulf of Guinea, GoG), using long-term offshore observation (sea-surface measured) data captured at five offshore synoptic stations in the GoG (see description of the dataset in section 2.1). In this work, the (i) spatio-temporal analysis of sea-surface wind observations at five offshore synoptic stations in the GoG, (ii) seasonal variations in wind speed and directions, (iii) evaluation of wind

shear, wind power, capacity factor, and accumulated energy outputs at seasonal and annual time scales for the selected commercial offshore wind turbines, and (iv) economic analyses of offshore wind power development using LCOE, were conducted.

2. Material and methods

In assessing offshore wind resources along the GoG, the following aspects are of particular importance. In this section, the wind speed data and selection of sites, and the mathematical models adopted for this work, were comprehensively discussed.

2.1. Description of site and wind data

Continuous observations of sea-surface wind speed and direction at 30-minute intervals between 1979 and 2015 at five offshore observation stations in the GoG were used in this work. The offshore locations include Forcados (5.17° N, 5.18° E; on shallow water at the coast), Bonny (4.40° N, 7.14° E; on shallow water at the coast), Sea Eagle (4.80° N, 5.31° E; on deep water, 49 nautical miles off the shore of Warri, Nigeria), Bonga (4.56° N, 4.62° E; on deep water, 72 nautical miles off the shore of Warri, Nigeria), and Agbami (3.46° N, 5.56° E; on deep water, 131 nautical miles off the shore of Warri, Nigeria). Fig. 2 depicts the geographical locations of the sites in the Southern Atlantic Ocean bordering the coastline of Nigeria. The measurements were taken at 10 m to 22 m above mean sea level, at every 1- to 30-minute intervals. At

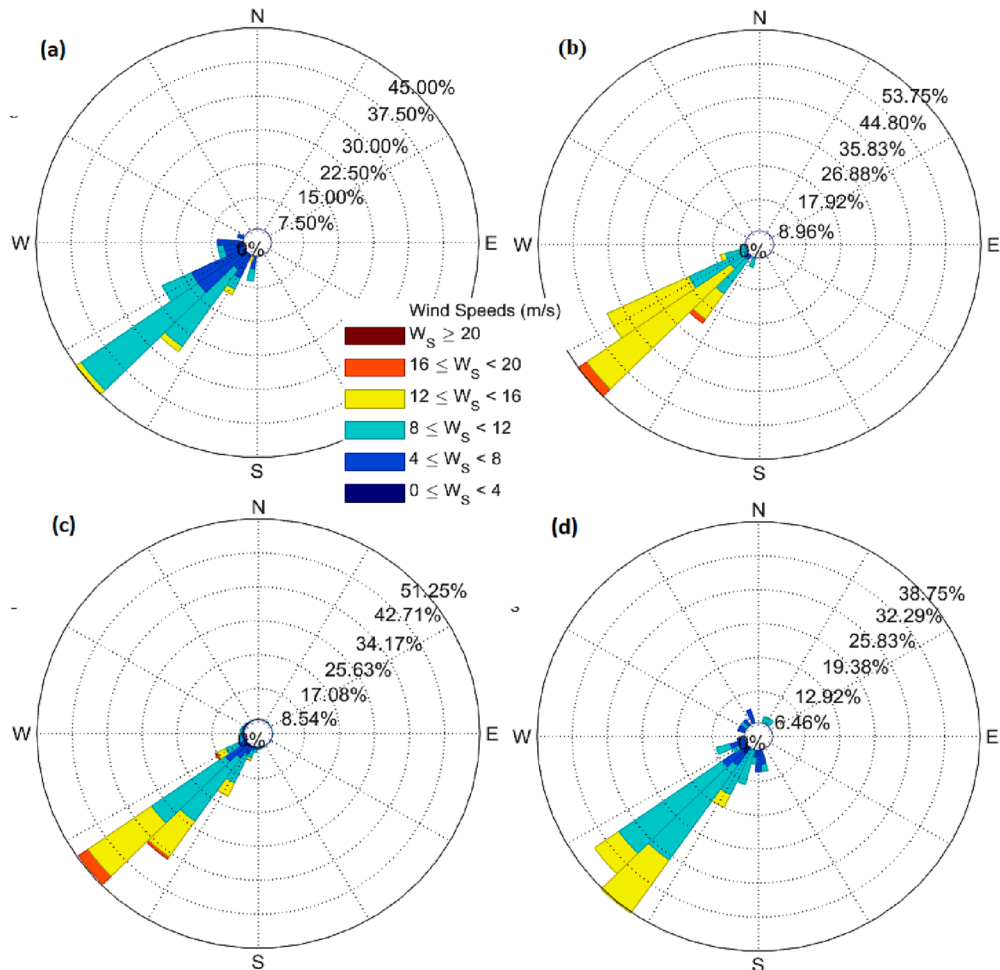


Fig. 4. Seasonal (DJF, MAM, JJA, & SON) variations in wind rose compass distribution of sea-surface wind speed at the deepest offshore observation station (Agbami) during the study period: (a) December to February, DJF; (b) March to May, MAM; (c) June to July, JJA; and (d) September to November, SON seasons.

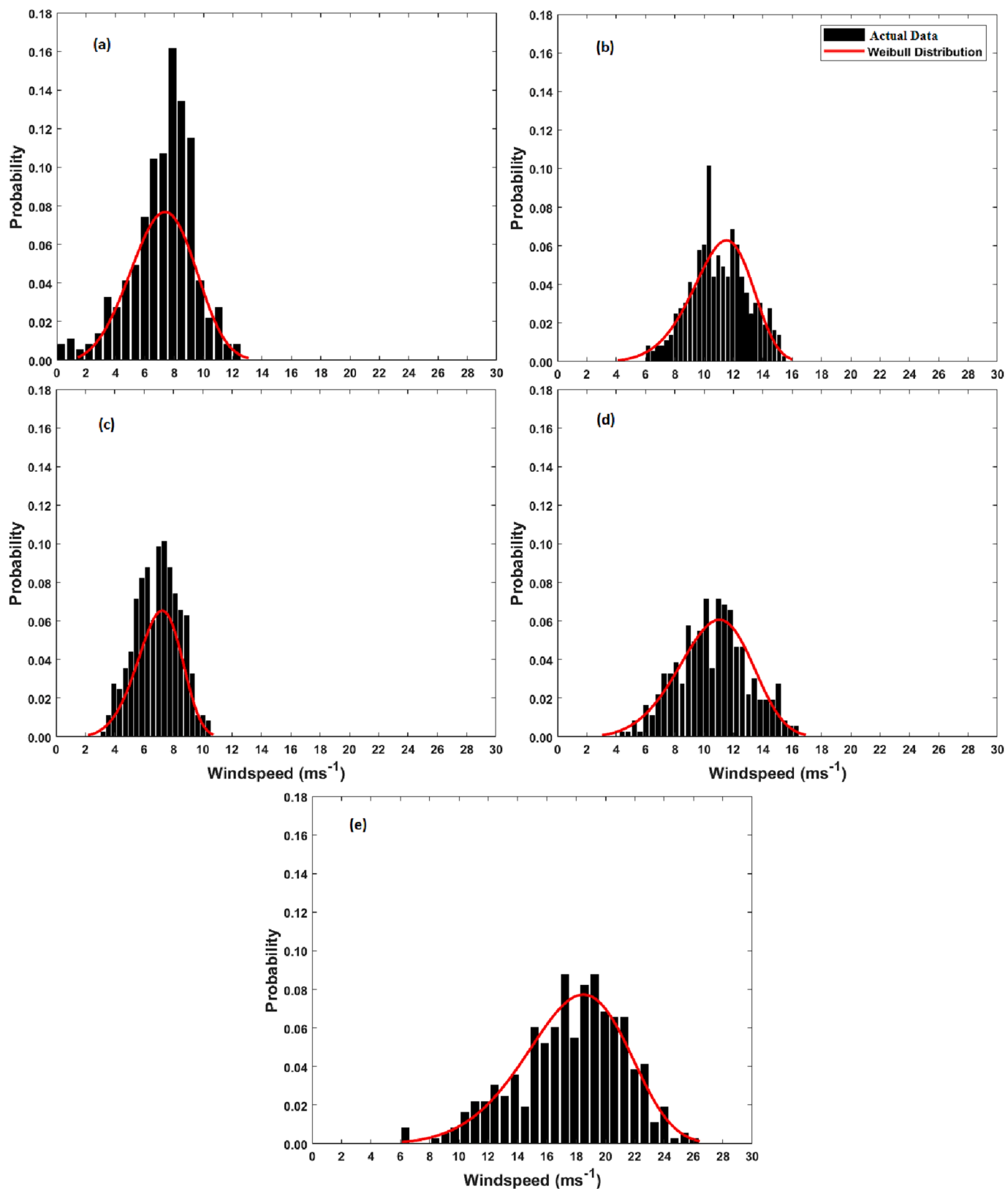


Fig. 5. Weibull frequency distribution of hourly mean wind speed at 100 m hub height: (a) Forcados, (b) Sea Eagle, (c) Bonny, (d) Bonga and (e) Agbami stations during the study period.

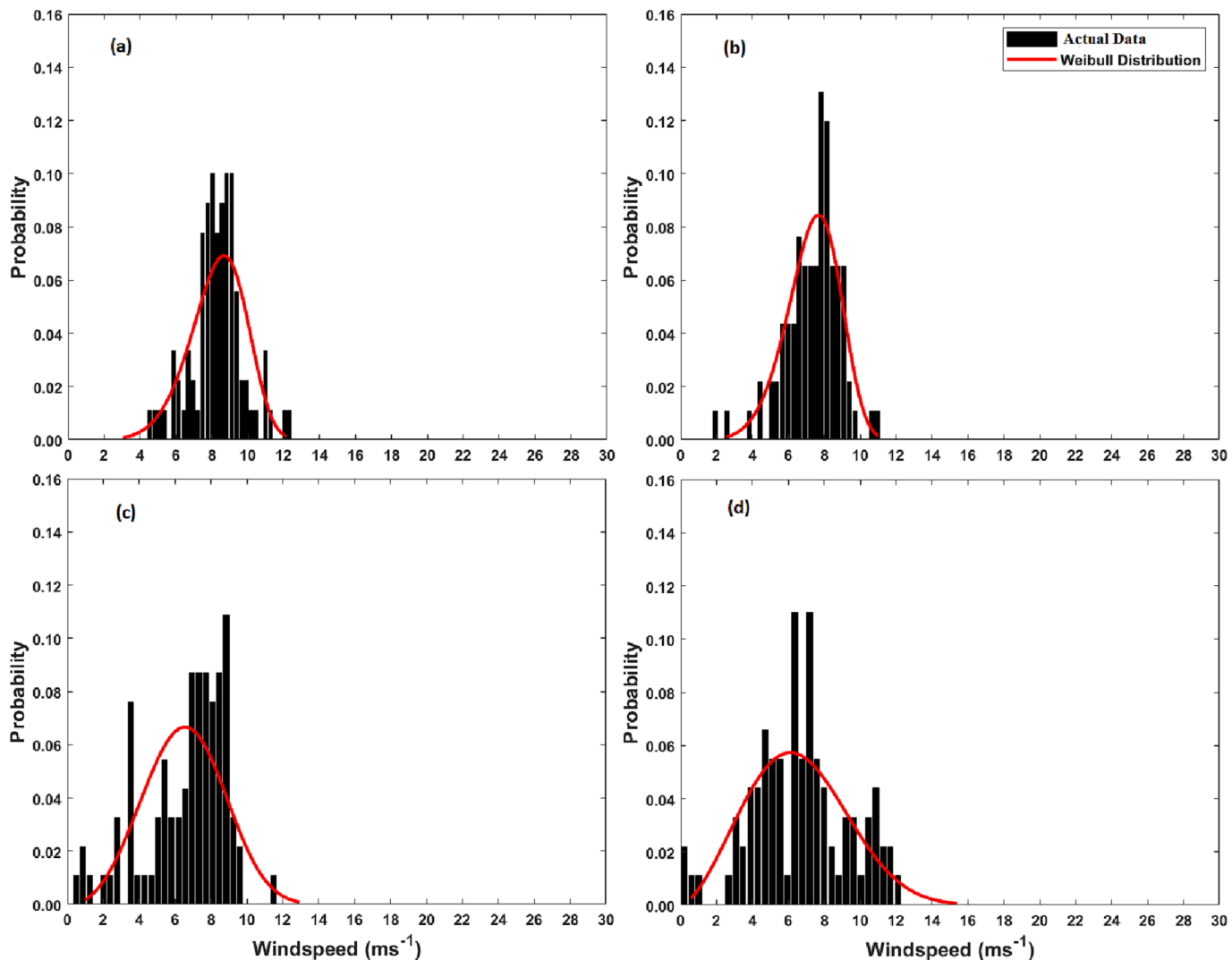


Fig. 6. Weibull frequency distribution of seasonal wind speed (100 m) at Forcados station during the study period: (a) December to February, DJF; (b) March to May, MAM; (c) June to July, JJA; and (d) September to November, SON seasons.

the Bonny site, an S2000 mechanical meteorological station manufactured by SIAP Bologna having serial number SIAP-1 was used for the continuous measurements of sea-surface wind speed and direction during the special observation period. At Sea Eagle, OMC 150 weather instrument manufactured by Observator with serial number 15000483 was used. At the other three stations i.e., Forcados, Agbami, and Bonga, RMS-2 meteorological recording station by NBA (CONTROLS) Limited with serial number NBA-1 was deployed for the wind data measurements.

The data were analyzed to examine daily to seasonal variations in hourly surface wind speed and directions. The Weibull distribution of wind speed and power density at 100 m hub height were also examined. Wind shear and capacity factor for seven commercial offshore wind turbines were computed for each site at seasonal and annual time scales. The selected wind turbines are V236-15.0 MW, V164-10.0 MW, V174-9.5 MW, V164-9.5 MW, V117-4.2 MW, GE (3.6sl), and Siemens (SWT113), and are found to be suitable for diverse offshore terrains. The technical characteristics of the selected wind turbines (such as hub height, rated power, cut-in wind speed, cut-out wind speed, etc.) are presented in Table 1.

2.2. Wind characteristics and Weibull parameters

The Weibull parameter for wind speed is given by the probability density function [40], and cumulative probability function [40] in Equations (1) and (2):

$$f(V) = \left(\frac{k}{c}\right)\left(\frac{V}{c}\right)^{k-1} \exp\left[-\left(\frac{V}{c}\right)^k\right] \quad (1)$$

$$F(V) = 1 - \exp\left[-\left(\frac{V}{c}\right)^k\right] \quad (2)$$

c and k are the Weibull scale and shape parameters, respectively, in Eqs. (3) and (4):

$$k = \left(\frac{\delta}{V_j}\right)^{-1.086} \quad (1 \leq k \leq 10) \quad (3)$$

$$c = \frac{V_j}{\Gamma(1 + \frac{1}{k})} \quad (4)$$

δ = standard deviation, V_j = mean wind speed (m/s), and $\Gamma(z)$ = gamma function of (z).

Furthermore, the statistical evaluation of the performance of the

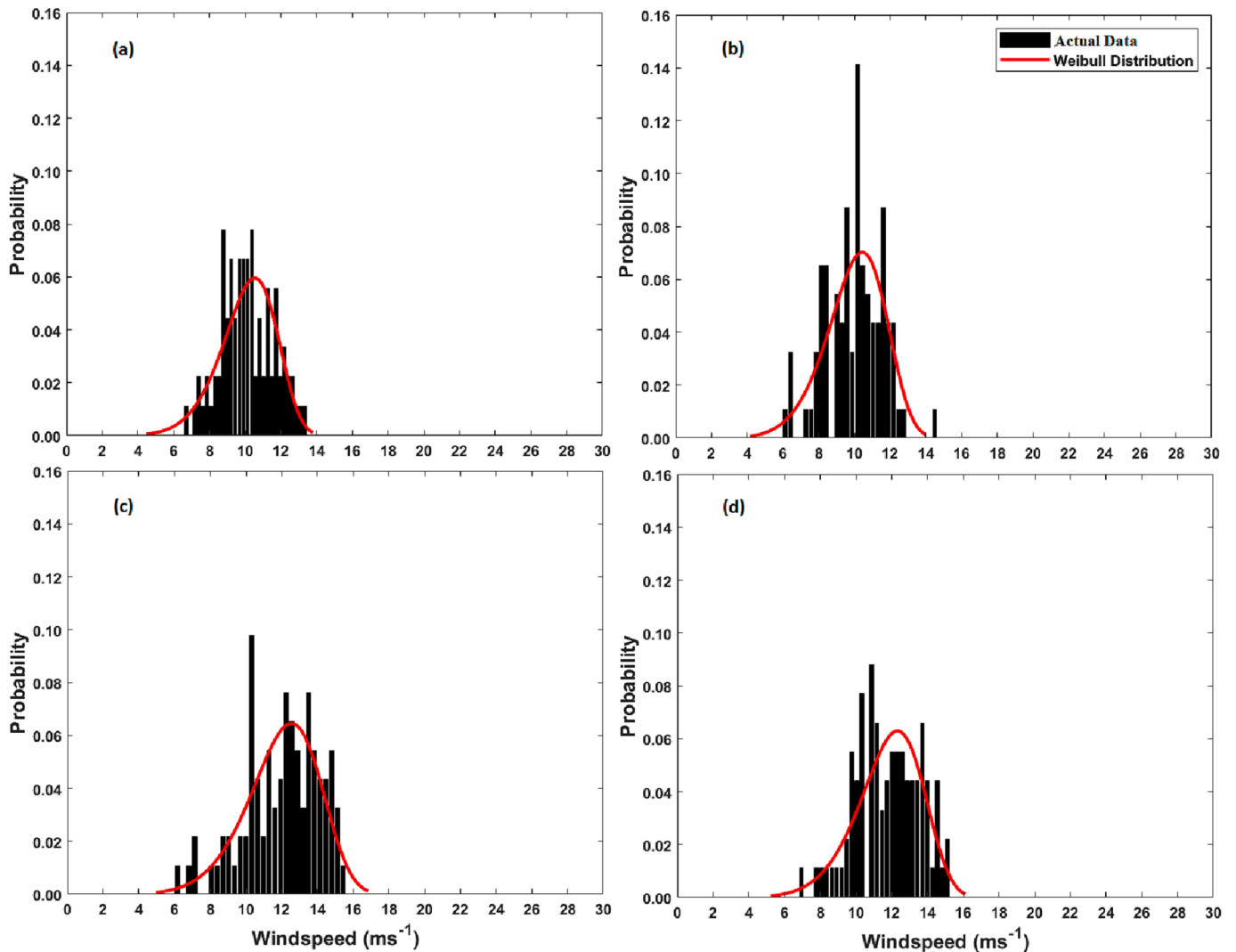


Fig. 7. Weibull frequency distribution of seasonal wind speed (100 m) at Sea Eagle station during the study period: (a) December to February, DJF; (b) March to May, MAM; (c) June to July, JJA; and (d) September to November, SON seasons.

Weibull distribution function in replicating the wind speed was carried out using indices including correlation coefficient (r) [41], Chi-square (χ^2) [42], root mean square error (RMSE), BIAS, and PBIAS [41]. These indices were estimated using the empirical Eqs. (5) to (9).

$$r = \frac{\sum_{i=1}^n (y_i - \bar{y})(x_i - \bar{x})}{\sqrt{\sum_{i=1}^n (x_i - \bar{x})^2 \sum_{i=1}^n (y_i - \bar{y})^2}} \quad (5)$$

$$\chi^2 = \frac{\sum_{i=1}^n (y_i - x_i)^2}{x_i} \quad (6)$$

$$RMSE = \left[\frac{1}{N} \sum_{i=1}^N (y_i - x_i)^2 \right]^{\frac{1}{2}} \quad (7)$$

$$BIAS = \frac{\sum_{i=1}^N (y_i - x_i)}{N} \quad (8)$$

$$PBIAS = 100 \times \frac{\sum_{i=1}^N (y_i - x_i)}{\sum_{i=1}^N (y_i)} \quad (9)$$

where y_i is the i th measured or actual data, x_i is the i th predicted wind data with the Weibull distribution, and N is the number of observations.

2.3. Wind speed extrapolation at different hub heights

The wind speed at a particular hub height is essential for wind power applications. Hence, measured wind speeds at the known height are modified to that at the required height using the Power law [25]:

$$\frac{V}{V_o} = \left(\frac{h}{h_o} \right)^\alpha \quad (10)$$

V = wind speed at the required hub height (h), V_o = wind speed at measured height (h_o), and α = surface roughness coefficient. Often time, the Weibull parameters obtained at measured height are extrapolated to the hub heights using the expressions in Eqs. (11) and (12) since the exact value of the surface roughness coefficient is not always freely available [26].

$$c(h) = c_o \left(\frac{h}{h_o} \right)^\alpha \quad (11)$$

$$k(h) = k_o \left[1 - 0.088 \ln \left(\frac{h_o}{10} \right) \right] / \left[1 - 0.088 \ln \left(\frac{h}{10} \right) \right] \quad (12)$$

c_o = scale factor, k_o = shape factor, h_o = measurement height, h = hub height. The exponent ' α ' is expressed as:

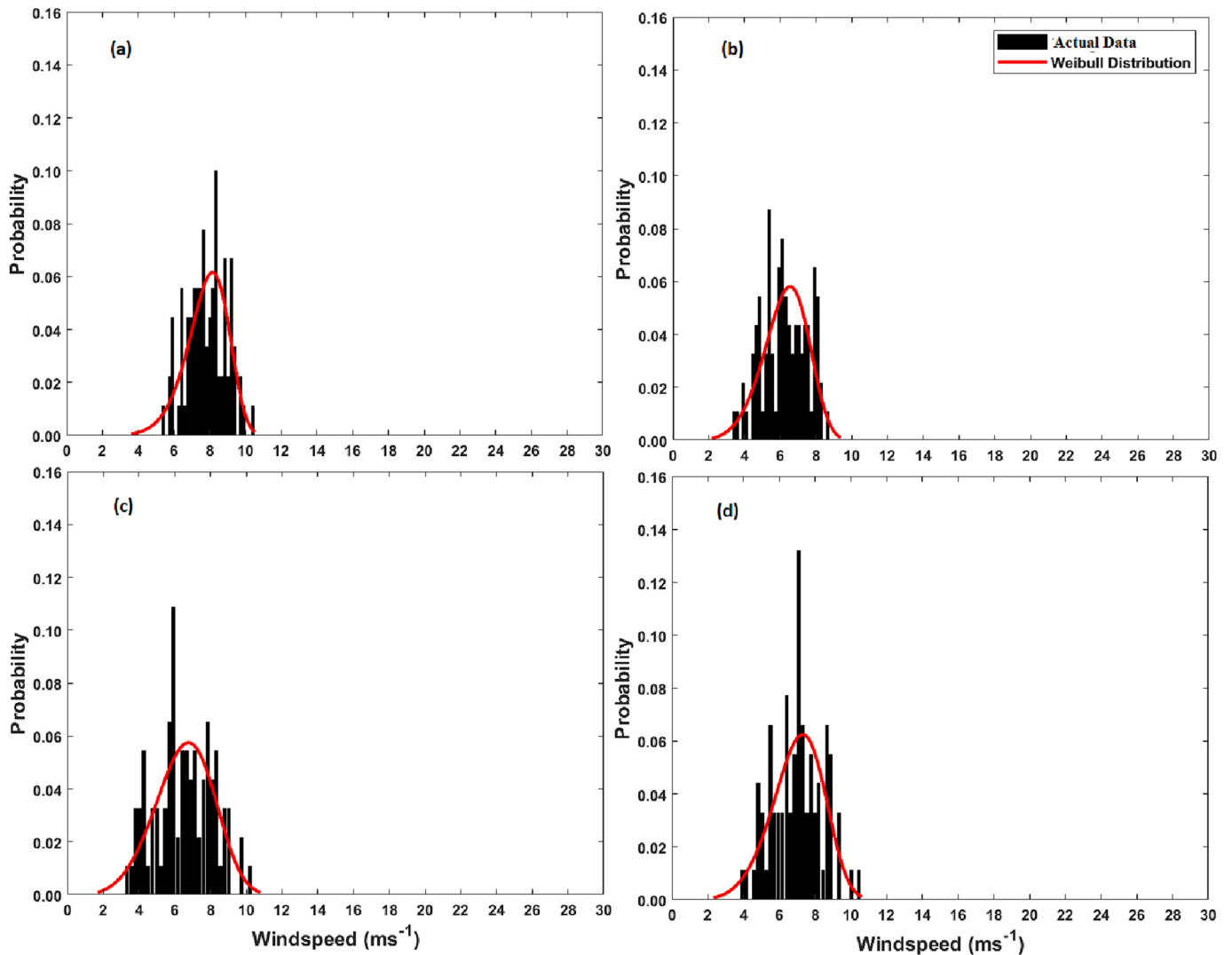


Fig. 8. Weibull frequency distribution of seasonal wind speed (100 m) at Bonny station during the study period: (a) December to February, DJF; (b) March to May, MAM; (c) June to July, JJA; and (d) September to November, SON seasons.

$$\alpha = [0.37 - 0.088\ln(c_o)] / \left[1 - 0.088\ln\left(\frac{h}{10}\right) \right] \quad (13)$$

2.4. Estimation of wind power, capacity factor, and economic analysis of the wind turbines

The wind power density via the Weibull distribution function is given as:

$$p(V) = \frac{P(V)}{A} = \frac{1}{2} \rho c^3 \Gamma(1 + \frac{3}{k}) \quad (14)$$

$p(V)$ = wind power density (W/m^2), $P(V)$ = wind power (W), ρ = air density, A = rotor blades swept area (m^2).

The mean wind shear ($\text{WSH (s}^{-1}\text{)}$) for the selected wind turbines at the offshore observation stations was estimated using the expression given in Eq. (15):

$$\text{WSH} = \frac{c_1 - c_0}{h - h_0} \quad (15)$$

The mean power output ($P_{e,mean}$) and capacity factor (C_f) of any installed wind turbine can be calculated using the expressions in Eqs. (16) and (17) [40]:

$$P_{e,mean} = P_{eR} \left(\frac{e^{-(\frac{V_c}{c})^k} - e^{-(\frac{V_f}{c})^k}}{\left(\frac{V_c}{c}\right)^k - \left(\frac{V_f}{c}\right)^k} - e^{-\left(\frac{V_f}{c}\right)^k} \right) \quad (16)$$

$$C_f = \frac{P_{e,mean}}{P_{eR}} \quad (17)$$

P_{eR} = rated electrical power of the turbine, V_c = cut-in wind speed, V_r = rated wind speed, V_f = cut-off wind speed.

The accumulated annual energy output (E_o) is given by:

$$E_o = P_{e,mean} \times 8760 \text{ (kWh)} \quad (18)$$

An estimation of the unit cost of energy using the LCOE method is expressed in [40] as:

$$\text{LCOE} = \frac{\text{CRF}}{E_{WT}} (C_I + C_{om(esc)}) \text{ USD/kWh} \quad (19)$$

C_I = total investment cost, $E_{WT} (= 8760P_{eR}C_f)$ = annual energy output of wind turbine (kWh),

CRF = capital recovery factor, $C_{om(esc)}$ = present worth of the annual cost throughout turbine life [40]:

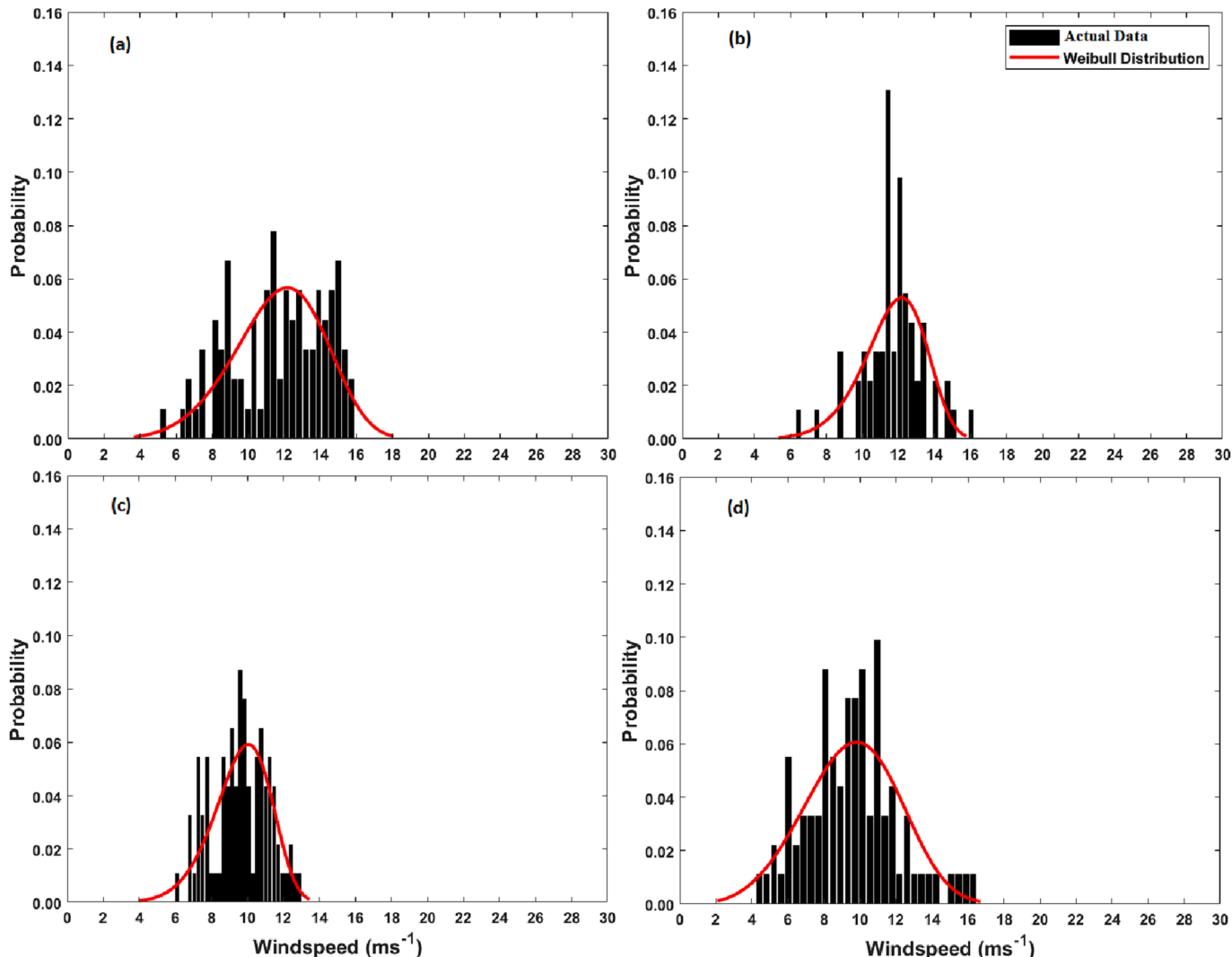


Fig. 9. Weibull frequency distribution of seasonal wind speed (100 m) at Bonga station during the study period: (a) December to February, DJF; (b) March to May, MAM; (c) June to July, JJA; and (d) September to November, SON seasons.

$$C_I = C_{dev} + C_{turb} + C_{found}(d) + C_{trans}(D) + C_{inst}(D) + C_{decom} \quad (20)$$

C_I in Eq. (20) are calculated on a per-megawatt (1/MW) basis for each site [43]. Development costs (C_{dev}) and turbine costs (C_{turb}) depend only on wind farm capacity. Foundation costs (C_{found}) are dependent on water depth (d). Transmission costs (C_{trans}) and installation costs (C_{inst}) depend on each site's distance (D) to the nearest coastline. Decommissioning costs (C_{decom}) are calculated as a proportion of installation costs [43].

$$CRF = \frac{(1+r)^n r}{(1+r)^n - 1} \quad (21)$$

$$C_{om(esc)} = \frac{Com}{r - e_{om}} \left(1 - \left(\frac{1 + e_{om}}{1 + r} \right)^n \right) \text{USD/year} \quad (22)$$

C_{om} = operation and maintenance cost for the first year, e_{om} = escalation of operation and maintenance, n = life of turbine, r = discount rate.

The costs of MWh of energy produced using LCOE by the selected turbines were evaluated by taking the following assumptions into consideration:

- a) From the manufacturers, turbine lifetime (n) is taken as 25 years (see Table 1).

- b) The discount rate is taken to be 9.4% for a large-scale project.
- c) The price of the selected wind turbines is given in Table 1.
- d) The operation and maintenance costs (C_{om}) was assumed to be 25% of the offshore wind turbine's annual cost. In Taboada et al. [44], larger wind turbines are found to generate much greater uncertainties; hence, C_{om} represent a large portion of the total life cycle cost, making it approximately 22 to 40% of the annual cost of the offshore wind turbine.
- e) The escalation rate of operation and maintenance ($C_{om(esc)}$) was assumed to be 3.5% (for sites in shallow waters with fixed-bed substructure) and 4.0% (for sites in deep waters with floating substructure). This amount could compensate for increasing workers' salary.
- f) Other initial costs, i.e., installation costs, grid integration, substructure, and foundation, were assumed to be 35% of the wind turbine cost (for sites in shallow waters) and 40% of the wind turbine cost (for sites in deep waters). These assumptions align with observations in Stehly et al., [45].
- g) The wind turbines were further assumed to produce the same energy output each year during their lifetime.
- h) The LCOE categories for the representative offshore wind projects in this work only consider the turbine capital expenditure, balance of system capital expenditure, and operation and maintenance (C_{om}) costs because there are limited empirical data on more detailed

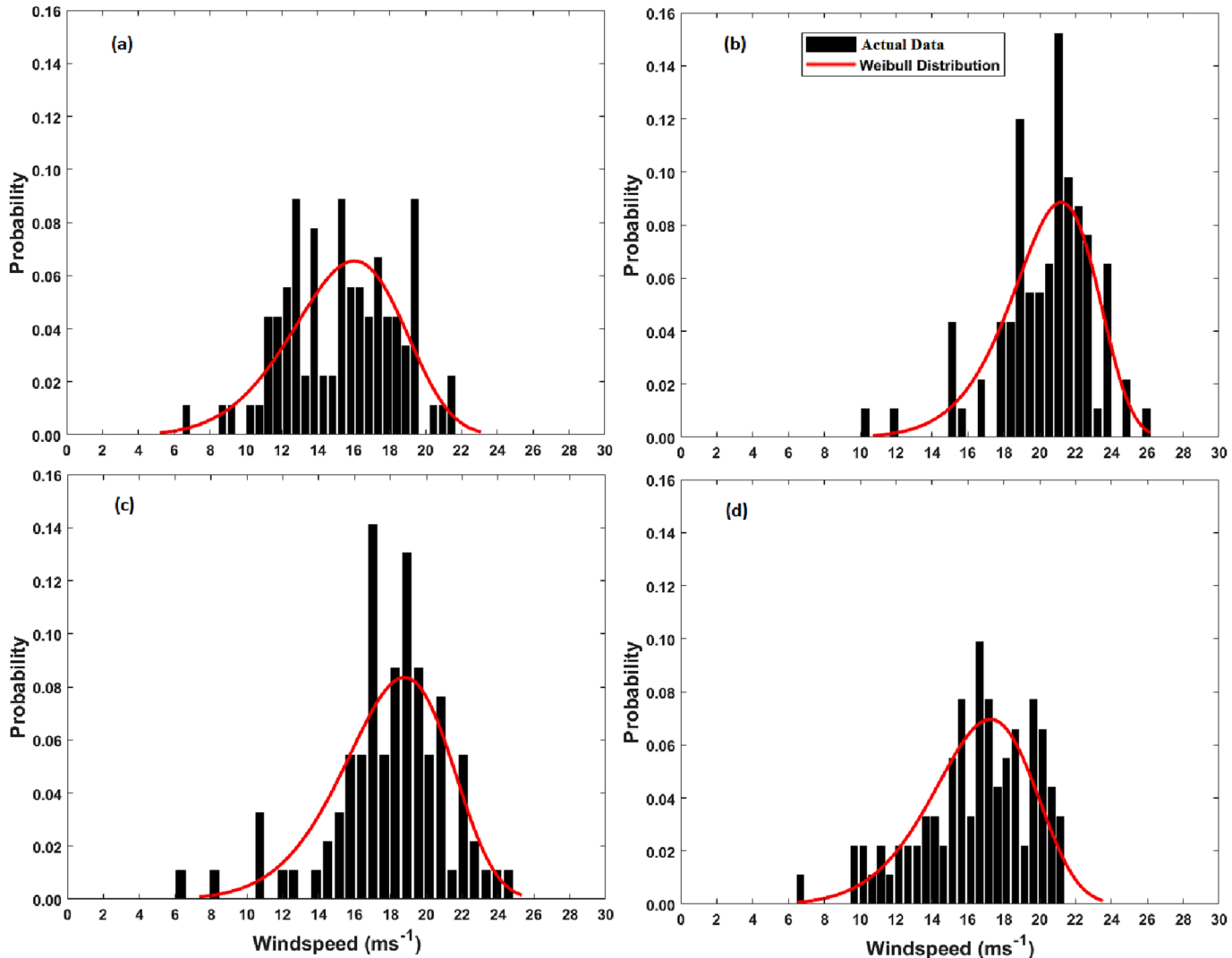


Fig. 10. Weibull frequency distribution of seasonal wind speed (100 m) at Agbami station during the study period: (a) December to February, DJF; (b) March to May, MAM; (c) June to July, JJA; and (d) September to November, SON seasons.

Table 3

Comparison of the measured probability distribution of wind speeds with the Weibull probability distribution at the selected offshore sites.

Periods/ Seasons	Indices	Offshore Sites				
		Forcados	Sea Eagle	Bonny	Bonga	Agbami
DJF	r	0.941	0.984	0.987	0.990	0.987
	χ^2	0.143	0.034	0.027	0.162	0.247
	RMSE	1.099	0.588	0.460	1.306	1.864
	BIAS	0.122	-0.060	0.084	-1.135	-1.264
	PBIAS	1.463	-0.590	1.079	-9.757	-8.243
MAM	r	0.935	0.973	0.992	0.910	0.929
	χ^2	0.427	0.109	0.032	0.127	0.529
	RMSE	1.646	1.067	0.440	1.667	3.107
	BIAS	-1.006	0.350	-0.245	-1.821	-2.092
	PBIAS	-13.687	3.480	-3.897	-10.651	-10.294
JJA	r	0.948	0.976	0.989	0.985	0.930
	χ^2	0.315	0.186	0.057	0.036	0.789
	RMSE	1.373	1.417	0.621	0.589	3.510
	BIAS	-0.609	-1.182	0.338	-0.162	-2.348
	PBIAS	-9.227	-9.882	5.227	-1.674	-13.062
SON	r	0.970	0.985	0.982	0.967	0.963
	χ^2	0.225	0.101	0.067	0.219	0.613
	RMSE	1.179	1.056	0.696	1.510	2.927
	BIAS	-0.427	-0.752	0.274	0.832	-2.517
	PBIAS	-6.458	-6.359	3.935	8.672	-15.246
All Seasons	r	0.966	0.976	0.969	0.980	0.989
	χ^2	1.221	0.181	0.197	0.938	0.308
	RMSE	2.810	1.396	1.166	3.127	2.230
	BIAS	-1.448	0.404	-0.495	-2.444	-0.076
	PBIAS	-13.295	3.896	-6.689	-13.984	-0.469

r = Correlation Coefficient, χ^2 = Chi-square, RMSE = Root mean square error, BIAS = Mean bias or error, PBIAS = Percentage mean bias or error.

DJF = December – February, MAM = March – May, JJA = June – July, SON = September – November.

system cost breakdown, including lease price, plant commissioning, decommissioning, contingency, construction finance, insurance during construction, development, engineering management, port and staging, logistics, transportation for the fixed-bed and floating offshore plant, needed for offshore wind projects in the GoG. These financial cost components are not included as input in the computation of LCOE.

The sensitivity analyses of wind total LCOE to key input parameters were examined to address evolving cost assumptions. The values of these parameters were varied within realistic ranges. The discount rate was varied by $\pm 4\%$ point of the base value, while the other variables (including total investment cost, turbine lifetime, operation and maintenance cost for first year, and escalation of operation and maintenance) were moved $\pm 20\%$ of their base value.

3. Results and discussion

This section presents the technical and economic assessments of the offshore wind at the GoG.

3.1. Wind speed and directions of sea-surface wind at the offshore observation stations

Table 2 provides a summary of the hourly mean sea-surface wind speed characteristics at the selected offshore stations across the four astronomical seasons (namely, December to February, DJF; March to May, MAM; June to July, JJA; September to November, SON) in the GoG, during the special observation period. The results in **Table 2** demonstrated large spatio-temporal variations in wind speed over the selected offshore sites in the GoG. For example, maximum wind speeds obtained at the sites were 30.8 ms^{-1} (Agbami), 14.4 ms^{-1} (Sea Eagle), 13.3 ms^{-1} (Bonga), 13.0 ms^{-1} (Forcados), and 9.0 ms^{-1} (Bonny). It was

further revealed that the wind speeds increased from the shallowest (coastal site of Bonny) to the deepest offshore site (Agbami). This observation supports the finding in previous work that offshore wind speeds vary with coastline orientation, water depth, air-sea temperature differences, latitude (related to the magnitude of solar radiative forcing) [36], distance from the coastal discontinuity, and fetch [37]. Tian et al. [46] also reported higher sea surface wind speed over deeper offshore locations than nearby onshore locations.

The seasonal analysis of mean wind speed revealed high variability in wind speeds across DJF, MAM, JJA, and SON seasons, in the GoG (**Table 2**). For example, maximum wind speeds were obtained in DJF or MAM seasons in all the sites. The standard deviations of the wind speed ranged between 1.26 and 1.52 ms^{-1} in the shallowest coastal site (Bonny) and between 3.40 and 3.82 ms^{-1} in the farthest offshore deep-sea site (Agbami). Furthermore, the coefficient of variation (i.e., the ratio of the standard deviation to the mean wind speed) was largely greater than 30% in virtually all the sites and seasons (**Table 2**). These indicate large and significant variability in wind speed at the GoG. Similarly, the Weibull shape and scale factors (k_0 and c_0) closely followed the same patterns of spatio-temporal variations in wind speed. The performance evaluations of the Weibull distribution function in replicating the actual wind speed are presented in the subsequent subsection.

The seasonal variations in the wind rose distribution of sea-surface wind speed at Bonny (the shallowest site) and Agbami (the deepest site) offshore observation stations are presented in [Figs. 3 and 4](#), respectively. The findings revealed the dominance of south-westerly (SW) across the locations (stronger in deeper offshore sites than the shallow locations) all year round, with the peaks in the JJA season. For instance, in the DJF season, SW dominated with speed magnitudes ranging from 2 to 8 ms^{-1} at Bonny and 4 to 16 ms^{-1} at Agbami ([Fig. 3a](#) and [4a](#)). In MAM and JJA seasons, the dominance of SW became more pronounced, thus signalling the peak of the West African Monsoon (WAM) with increasing speed having prevalent magnitudes of 3 to 8 ms^{-1} and 8 to 20 ms^{-1} at Bonny and Agbami, respectively ([Fig. 3b-c](#) and [4b-c](#)). The seasons coincide with the peak of convective precipitation (i.e., WAM) that principally dictates the regional climate of West Africa [47]. The dominance of SW subsides a little in the SON season with prevalent magnitudes of 2 to 8 ms^{-1} and 4 to 16 ms^{-1} at Bonny and Agbami, respectively. The results suggested that the most favourable site for offshore wind energy potential is Agbami, with probable hourly wind speeds ranging between 16.2 and 21.6 ms^{-1} . In addition, it is observed that Agbami is the most suitable offshore site for wind power exploitation, with the maximum wind energy potential in the MAM season.

3.2. Weibull frequency distribution

Fig. 5 illustrates the Weibull frequency distribution of mean hourly wind speed at 100 m hub height above the mean sea level (msl) over each of the selected offshore sites in the GoG. The peaks of the Weibull frequency distributions correspond to the probable wind speed with the highest counts or probability at each of the monitoring sites. Thus, the results revealed that the probable hourly wind speed was 7.3 , 11.8 , 7.1 , 11.2 and 18.5 ms^{-1} at Forcados, Sea Eagle, Bonny, Bonga, and Agbami, respectively. The ranges of the frequency distribution of wind speed at 100 m above msl were 1.7 – 12.9 ms^{-1} (Forcados), 4.0 – 16.0 ms^{-1} (Sea Eagle), 2.2 – 10.5 ms^{-1} (Bonny), 3.0 – 16.8 ms^{-1} (Bonga) and 6.4 – 26.3 ms^{-1} (Agbami).

The seasonal variations in the Weibull distribution of wind speed at 100 m height at Forcados, Sea Eagle, Bonny, Bonga, and Agbami are presented in [Figs. 6 to 10](#). The probable hourly wind speed at Forcados coastal site were 8.9 , 8.1 , 6.3 , and 6.0 ms^{-1} during DJF, MAM, JJA, and SON seasons, respectively ([Fig. 6](#)). The wind speed frequency distribution ranges at 100 m hub height are from 3.0 to 12.0 ms^{-1} in DJF and 0.5 to 15.5 ms^{-1} in SON season. The patterns of seasonal variations in the Weibull frequency distribution of wind speed were slightly different at

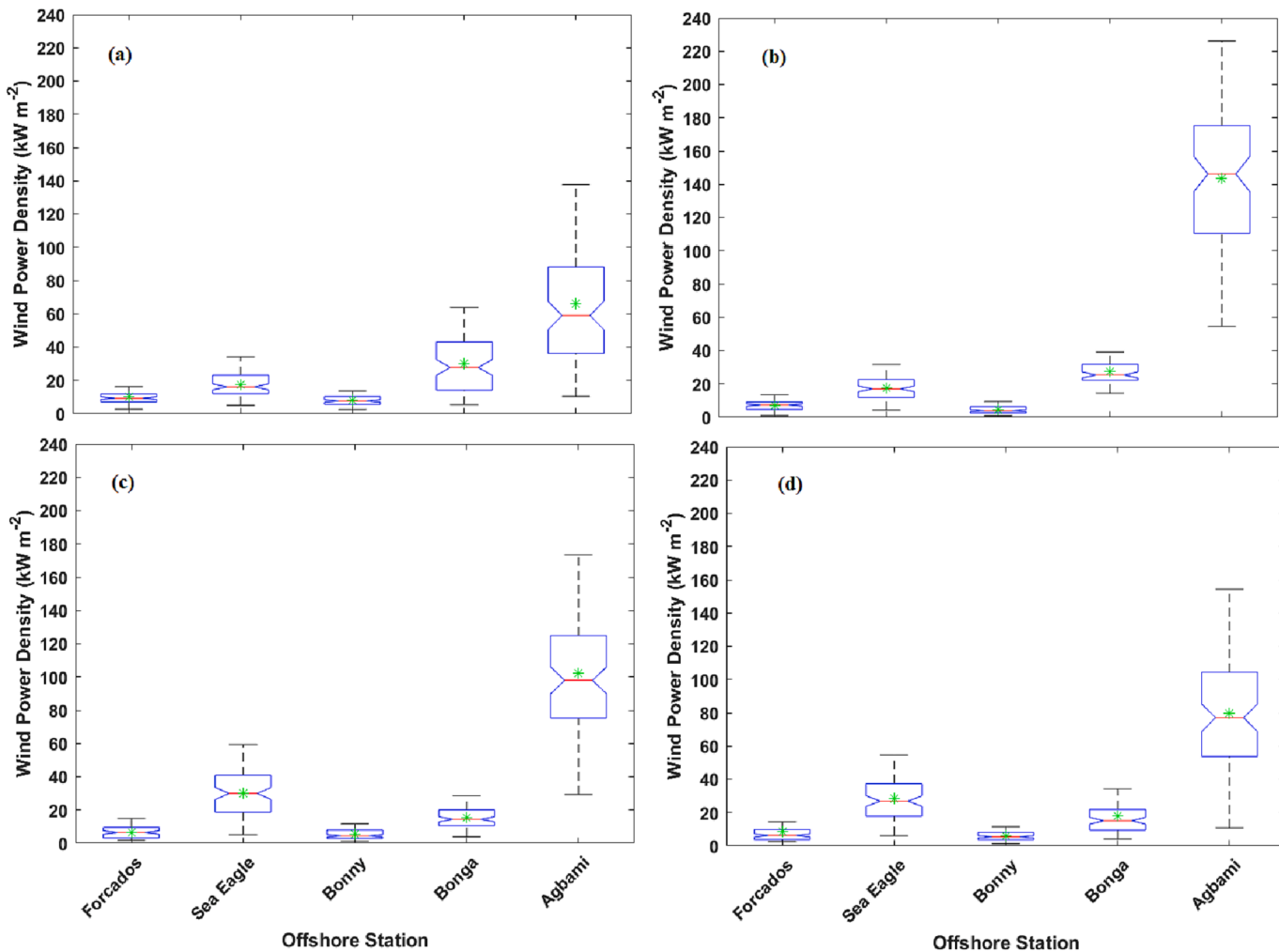


Fig. 11. Box plots of seasonal variations in wind power density (WPD) at 100 m above mean sea level [at the offshore observation stations]: (a) December to February, DJF; (b) March to May, MAM; (c) June to July, JJA; and (d) September to November, SON seasons.

Sea Eagle, Bonny, and Bonga (Figs. 7–9). However, at Agbami, the probable hourly wind speeds were 16.2, 21.6, 18.8, and 17.0 ms^{-1} during DJF, MAM, JJA, and SON seasons, respectively (Fig. 10). The frequency distributions at this site ranged between 5.0 and 23.0 ms^{-1} in DJF, 10.5 and 26.0 ms^{-1} in MAM, 7.0 and 25.0 ms^{-1} in JJA, and 7.0 and 23.3 ms^{-1} in SON. The spatial and temporal variations in the patterns of the Weibull distribution were found to follow that of wind speed. The computed seasonal variations in the Weibull frequency distribution of wind speed at 100 m were found to differ from site to site during the study period.

The results of the performance evaluation of the Weibull distribution in predicting wind speed at the hub height are presented in Table 3. The findings demonstrated that the Weibull distribution is a good match with the measured/actual data. In all seasons, the correlation coefficients were relatively high ($0.97 \leq r \leq 0.98$) and significant. The Chi-square values ($0.2 \leq \chi^2 \leq 1.2$) and root mean square error ($1.2 \text{ ms}^{-1} \leq \text{RMSE} \leq 3.1 \text{ ms}^{-1}$) were relatively low. In general, the Weibull distribution slightly underestimated wind speed at the study sites. The estimated discrepancies between the actual wind data and the predictions by the Weibull with mean bias ($-0.08 \text{ ms}^{-1} \leq \text{BIAS} \leq -2.44 \text{ ms}^{-1}$) and percentage bias ($-0.47\% \leq \text{PBIAS} \leq -13.98\%$), were found to be relatively low and could be said to be satisfactory. In Moriasi et al., [48], model simulations could be adjudged as satisfactory if $\text{PBIAS} \leq \pm 25\%$. The performance of the Weibull distribution as suggested by the five indices also varied across the seasons with the best simulation in DJF at all locations.

3.3. Wind power density at 100 m above mean sea level

Fig. 11 represents the box and whisker diagrams of the seasonal variations in wind power density (WPD) at 100 m above msl. The lower part of the whisker provides the 25th percentile (i.e., the lower quartile), while the upper part is the 75th percentile (i.e., the upper quartile). The numerical difference between the lower and upper quartiles is known as the Interquartile Range (IR). A vertical and dotted black line passes through the box to indicate the minimum and maximum values. In contrast, the line that divides the box into two equal parts represents the 50th percentile (i.e., the median value). Finally, the green star represents the mean value. The results show that Agbami (the deepest offshore site) had the highest WPD in all seasons while Bonny (the shallowest coastal site) had the least (Fig. 11). Overall maximum mean WPD of 145 kW m^{-2} was obtained at Agbami, while Bonny had the minimum of 4.5 kW m^{-2} in the MAM season. The widest (177 kW m^{-2}) and the shortest (129 kW m^{-2}) range of WPDs were obtained in MAM and DJF seasons, respectively, at Agbami. On the other hand, the maximum range was 15 kW m^{-2} in DJF, while the minimum range was 10.5 kW m^{-2} in MAM at Bonny. The highest and the lowest IR values were 66 kW m^{-2} (in MAM) and 36 kW m^{-2} (JJA), respectively, at Agbami site. At Bonny, the highest and the lowest IR values were found to be 6.3 kW m^{-2} (MAM) and 3.9 kW m^{-2} (JJA), respectively.

It is evident from these results that the mean WPD increased with hub height. In agreement with the observed wind speed patterns, the seasonal variations in WPD were high. In addition, the variability in

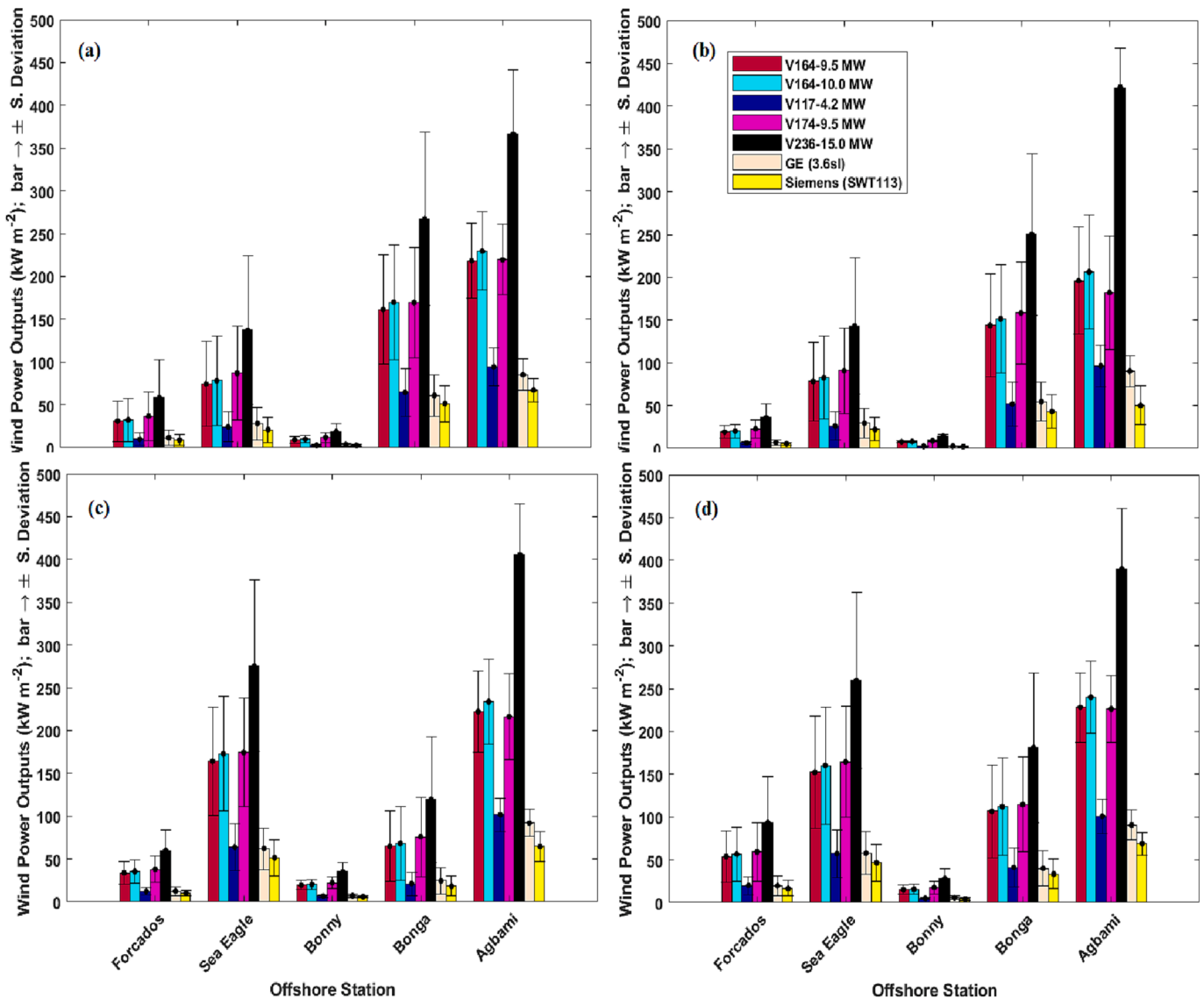


Fig. 12. Seasonal variations in the mean power outputs for the selected commercial wind turbines [at the offshore observation stations]: (a) December to February, DJF; (b) March to May, MAM; (c) June to July, JJA; and (d) September to November, SON seasons.

WPD regarding range and interquartile was higher in DJF or MAM than in other seasons. The results revealed that Agbami is the best region for harnessing wind energy generation in the GoG in all seasons. Bonny was the worst offshore location for wind energy generation, especially for grid-connected power development using large commercial offshore turbines.

3.4. Seasonal variations in mean power outputs, capacity factor, accumulated energy outputs, and wind shears

The seasonal variations in the estimated power outputs for the selected wind turbines are presented in Fig. 12. The results indicated that for all the selected offshore wind turbines at their respective hub heights, the offshore site with the highest wind power potential in all seasons was Agbami. Sea Eagle and Bonga closely followed Agbami, while the worst was at Bonny. The wind turbine type with the most promising power potential across the four seasons was V236-15.0 MW having maximum mean power outputs ranging from $363 \pm 70 \text{ kW m}^{-2}$ in DJF to $423 \pm 50 \text{ kW m}^{-2}$ in MAM season at Agbami (Fig. 12). The least power-yielding wind turbine type is Siemens (SWT113), with maximum power outputs of about 50 ± 20 (in MAM) to about 75 ± 10 (in other

seasons) at Agbami (Fig. 12).

Fig. 13 describes the seasonal variations in the wind turbines' capacity factor at the offshore observation stations. The values of the capacity factors for all the turbines at Agbami site ranged from 0.18 (or 18%) to 0.33 (33%) across the seasons (Fig. 13). Vestas V236-15.0 MW wind turbine had the highest capacity factor, followed by GE (3.6sl) at this location; the high-capacity factor observed with Vestas V236-15.0 MW turbine among the selected turbines, is due to its large swept areas and high hub-heights, thus enabling the machine to harvest more electricity from the same resource when compared with other selected turbines. On the other hand, at the Bonny location, the capacity factors for all the wind turbines were generally less than 0.035 (3.5%) in all seasons. The moderate capacity factor on the deep waters of the GoG align with the findings in IEA [49], where average capacity factors observed in regions nearer to the equator (e.g., in parts of West Africa and Southeast Asia), are found to be lower than the relatively high capacity factors of around 45–65% for regions in Europe, the North Sea, Baltic Sea, Bay of Biscay, Irish Sea, and Norwegian Sea, United States (40–55%), China (35–45%), Japan (35–45%), South America (50–65%), New Zealand (50–65%) and India (30–40%) IEA [49].

Furthermore, the seasonal mean variations in accumulated energy

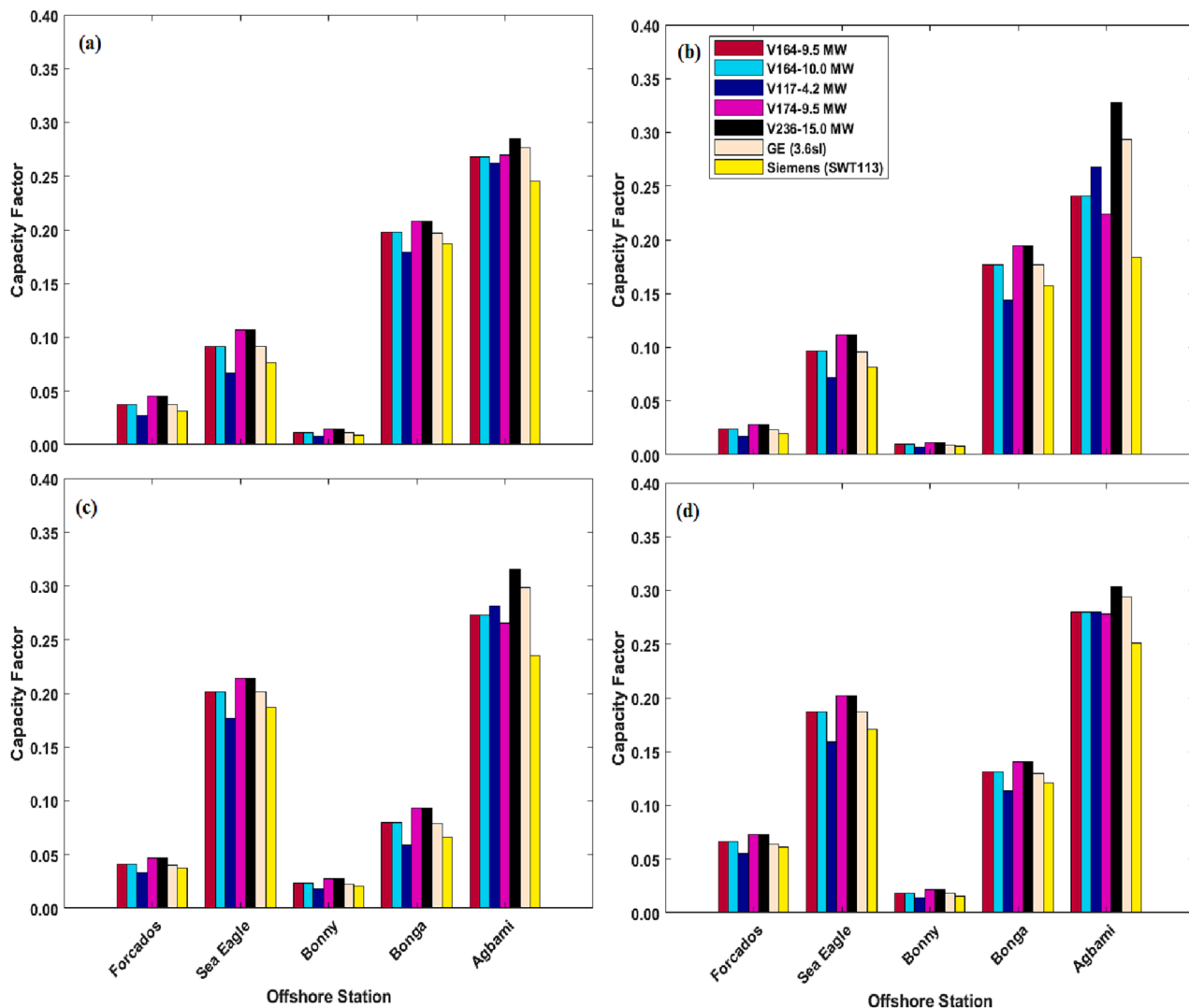


Fig. 13. Seasonal variations in capacity factor for the selected commercial wind turbines [at the offshore observation stations]: (a) December to February, DJF; (b) March to May, MAM; (c) June to July, JJA; and (d) September to November, SON seasons.

outputs for the selected wind turbines at the offshore observation stations are illustrated in Fig. 14. The highest accumulated energy outputs were obtained with V236-15.0 MW wind turbine at all sites (Fig. 14). The monthly mean energy output from V236 to 15.0 MW ranged from 540 kWh (in December, January and February) to 645 kWh (in June, July, and August) at Agbami. The lowest range of 10 to 98 kWh were obtained with Siemens (SWT113) wind turbine across the sites and seasons.

Wind shear profiles for the selected turbines at the offshore locations at different seasons are shown in Fig. 15. In all the seasons, the results showed that the highest and lowest wind shears (WSH) were found at Agbami and Bonny sites, respectively. This clearly suggested that the wind shear increases from the shallow to deeper offshore sites. The maximum wind shear ($0.12 \pm 0.013 \text{ s}^{-1}$) was obtained with Siemens (SWT113), while V236-15.0 MW had the least ($0.11 \pm 0.01 \text{ s}^{-1}$). This may be due to the fact that the vertical wind shear decreases with height; it must be noted that the hub height of Siemens (SWT113) is 80 m while that of V236-15.0 MW is 139 m (Table 1). The results also indicated that wind shear was weak in DJF but very strong in MAM and SON at all the sites. In agreement with the literature, the results suggested that wind shear had significant effects on the energy outputs from the wind turbines [50]. The findings established that the farthest site from the coast gives the largest average wind speed and power for all the selected

turbines.

3.5. Annual mean power outputs, capacity factor, accumulated energy outputs, and economic analysis of selected wind turbines

Fig. 16 summarises the results of the variations in annual mean power outputs, capacity factor, accumulated energy outputs, and LCOE for the selected wind turbines. Agbami site had the highest power outputs ranging from 1.0 ± 0.2 to $6.3 \pm 1.0 \text{ MWm}^{-2}$, followed by Sea Eagle (0.5 ± 0.2 to $3.3 \pm 1.2 \text{ MWm}^{-2}$), and then Bonga (0.4 ± 0.2 to $3.2 \pm 1.3 \text{ MWm}^{-2}$) (Fig. 16a). Bonny had the lowest annual average wind power with a range of values of 0.06 ± 0.02 to $0.2 \pm 0.1 \text{ MWm}^{-2}$ for all the selected wind turbines. In addition, V236-15.0 MW and Siemens (SWT113) turbines produced the highest and the lowest annual average wind power densities across the seasons and sites, respectively. This pattern of results suggests the deployment of large wind turbines (for example, V236-15.0 MW Vestas wind turbine) at deep offshore sites (like Agbami) for continual wind power generation.

Furthermore, the highest annual capacity factor (0.22–0.30) was obtained at Agbami and the lowest (~0.02) at Bonny for the selected wind turbines (Fig. 16b). The coastal site of Bonny having a significantly low-capacity factor was found to be non-windy and not able to propel large wind turbines (such as those selected for this work) economically.

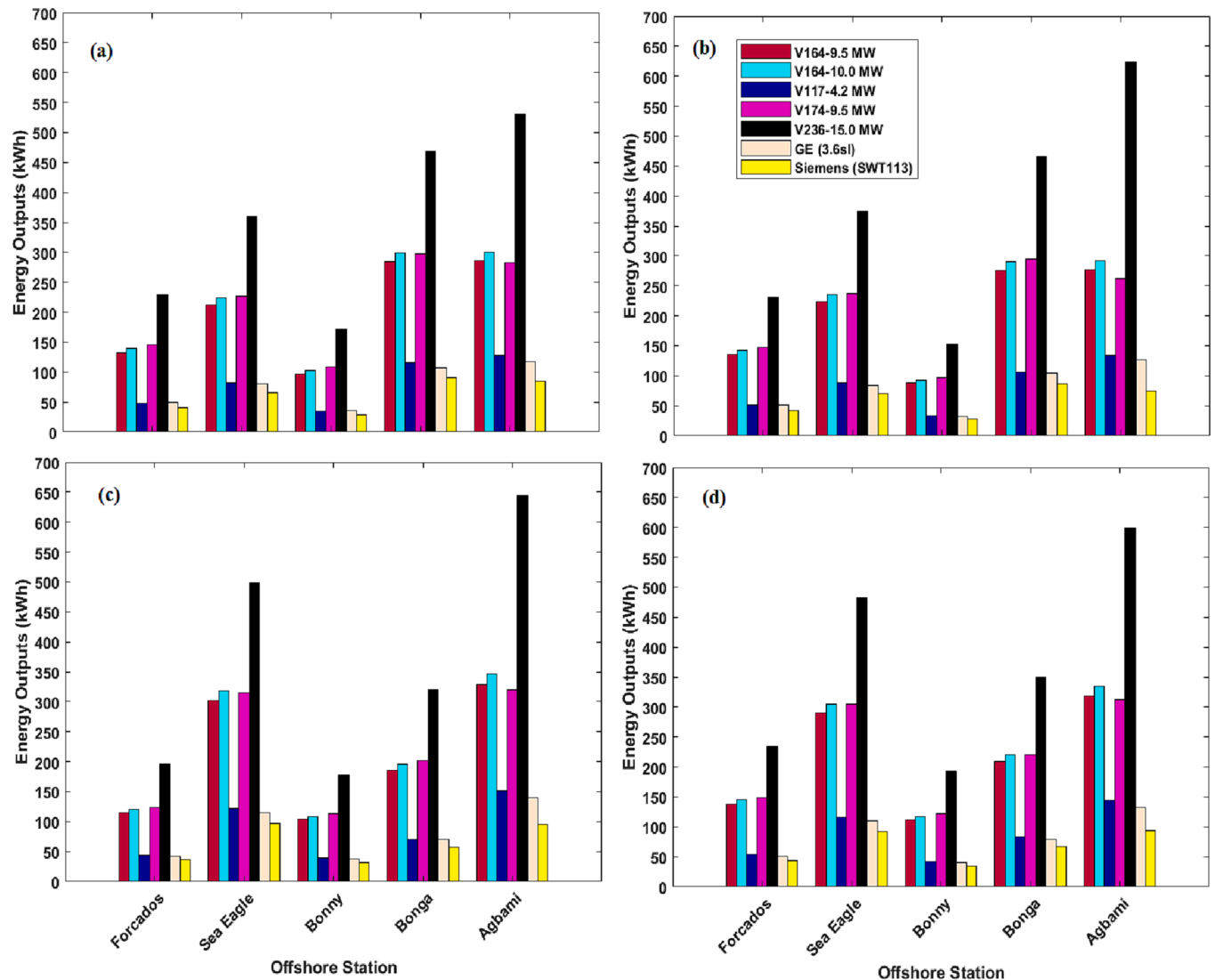


Fig. 14. Seasonal variations in accumulated mean energy outputs for the selected commercial wind turbines [at the offshore observation stations]: (a) December to February, DJF; (b) March to May, MAM; (c) June to July, JJA; and (d) September to November, SON seasons.

However, in previous work by Adaramola et al., [25], the coastal locations (Bonny and Forcados) were found to be exploitable using smaller wind turbines with lower-rated power. For instance, a 35 kW G-3120 wind turbine utilized in these locations was found to give a capacity factor of approximately 22.8% [25]. Hence, lower-rated wind turbines (like the G-3120 model and similar turbines) will be most suitable technically and economically for wind energy development in these locations. The annual accumulated energy output (23 – 152 MWh) at Agbami was the highest for all the wind turbines (Fig. 16c). It was also clear that, in all the sites, V236-15.0 MW and Siemens (SWT113) produced the highest and the lowest power density, respectively.

The economic analysis of the offshore turbines across the respective offshore locations was estimated using the LCOE (Equation (19)) and given in Fig. 16d. In this work, the LCOE was only considered for sites in the deep waters (Agbami, Bonga, and Sea Eagle) due to their moderate capacity factors (Fig. 16b and d). The coastal sites of Bonny and Forcados were excluded from the LCOE estimation due to the associated low-capacity factors (discussed in Section 3.5) for large offshore turbines of relatively high-rated capacities (utilized in this work). For the deep waters, it was evident that the farther the offshore site, the lower the LCOE. The farthest offshore location (Agbami) was the windiest, with the highest wind power. The LCOE was found to be lowest at Agbami for

all the selected offshore turbines, thus making the site to be economically viable for offshore wind exploitation; this is followed by Bonga, and Sea Eagle. The LCOE values ranged between 52.29 and 69.66 USD/MWh at Agbami with V236-15 MW and Siemens (SWT113), respectively, while it is between 101.19 and 131.55 USD/MWh at Bonga with V236-15 MW and V117-4.2 MW; the values were found between 101.48 and 137.12 USD/MWh at Sea Eagle with V236-15 MW and V117-4.2 MW, respectively (Fig. 16d). These estimated LCOE values compare favourably with historical LCOE of offshore wind and strike prices in recent auctions in Europe IEA [49]. Following the assumptions for the LCOE highlighted in Section 2.4, there are limited empirical data on a more detailed system cost breakdown. If empirical data are available for the listed financial cost components (Section 2.4) to estimate the LCOE for the respective locations and with the selected turbines, it should be noted that the LCOE values would be higher for these sites, than as currently reported.

The sensitivity analyses with the different offshore substructures (fixed-bottom and floating) are shown in Fig. 17. Among the selected turbines, Vestas V236-15 MW was adopted to be considered for sensitivity analysis at Bonny (shallow waters) for the fixed-bottom substructure (Fig. 17a) and Agbami (deep waters) for the floating substructure (Fig. 17b). The results showed that total investment cost

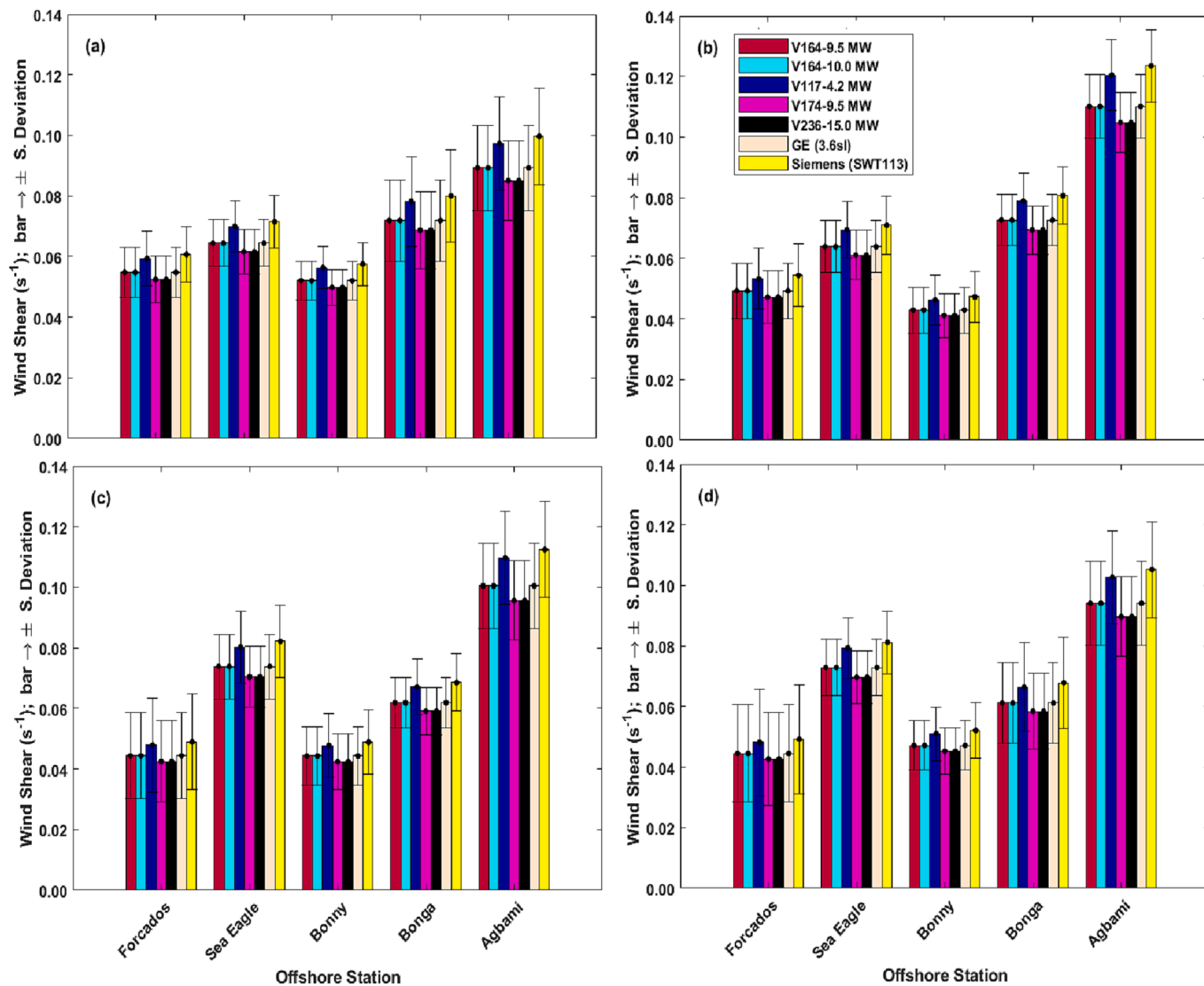


Fig. 15. Seasonal variations in wind shear profiles for the selected commercial wind turbines at the offshore observation stations: (a) December to February, DJF; (b) March to May, MAM; (c) June to July, JJA; and (d) September to November, SON seasons.

(C_I) was found to bear the most impact on the LCOE. C_I gave 62.1% and 61.9% on the LCOE for the floating and fixed-bottom turbines, respectively. This is followed by discount rate, which contributes about 33.1% to LCOE. Turbine lifetime, operation and maintenance cost for first year, and escalation of operation and maintenance, affect the LCOE range of either the fixed-bottom or floating offshore technology by about 4.2%, 0.5%, and 0.1%, respectively.

4. Conclusions

This present study assessed offshore wind potential in the Gulf of Guinea. Analyses of temporal and spatial wind data were carried out to discover the offshore observation station with the highest potential for wind energy exploitation. The following were concluded:

- There were large spatio-temporal variations in wind speed over the selected offshore sites in the GoG. The results revealed that the wind speeds increased from the shallowest (coastal location of Bonny) to the deepest offshore site (Agbami). It is established that Agbami, with probable hourly wind speeds ranging from 16.2 to 21.6 ms⁻¹, is the most suitable offshore site for wind exploitation with maximum wind power density (145 kW m⁻²) in March to May season.

- The findings established very good fits between the Weibull distribution and the actual wind data. Although the Weibull distribution slightly underestimated wind speed at the study sites, the estimated correlation coefficients were relatively high ($0.97 \leq r \leq 0.98$) and significant. The computed Chi-square ($0.2 \leq \chi^2 \leq 1.2$), root mean square error ($1.2 \text{ ms}^{-1} \leq \text{RMSE} \leq 3.1 \text{ ms}^{-1}$), mean bias ($-0.08 \text{ ms}^{-1} \leq \text{BIAS} \leq -2.44 \text{ ms}^{-1}$), and percentage bias ($-0.47\% \leq \text{PBIAS} \leq -13.98\%$), were found to be within satisfactory levels.
- The results established that the farthest site from the coast gives the largest average wind speed and wind power for all the selected turbines. The maximum wind shear ($0.12 \pm 0.013 \text{ s}^{-1}$) was obtained with Siemens (SWT113), while V236-15.0 MW had the least ($0.11 \pm 0.01 \text{ s}^{-1}$).
- The LCOE at Agbami was the lowest for all the selected turbines, thus, making the site to be the most economically viable location for offshore wind exploitation in the GoG. The findings also showed that total investment cost (C_I) (62.1% for floating and 61.9% for fixed-bottom turbines) was found to have the highest impact on the LCOE. It was further revealed that turbine lifetime, operation and maintenance cost for first year, and escalation of operation and maintenance, affect the LCOE of either the fixed-bottom or floating offshore technology by about 4.2%, 0.5%, and 0.1%, respectively.

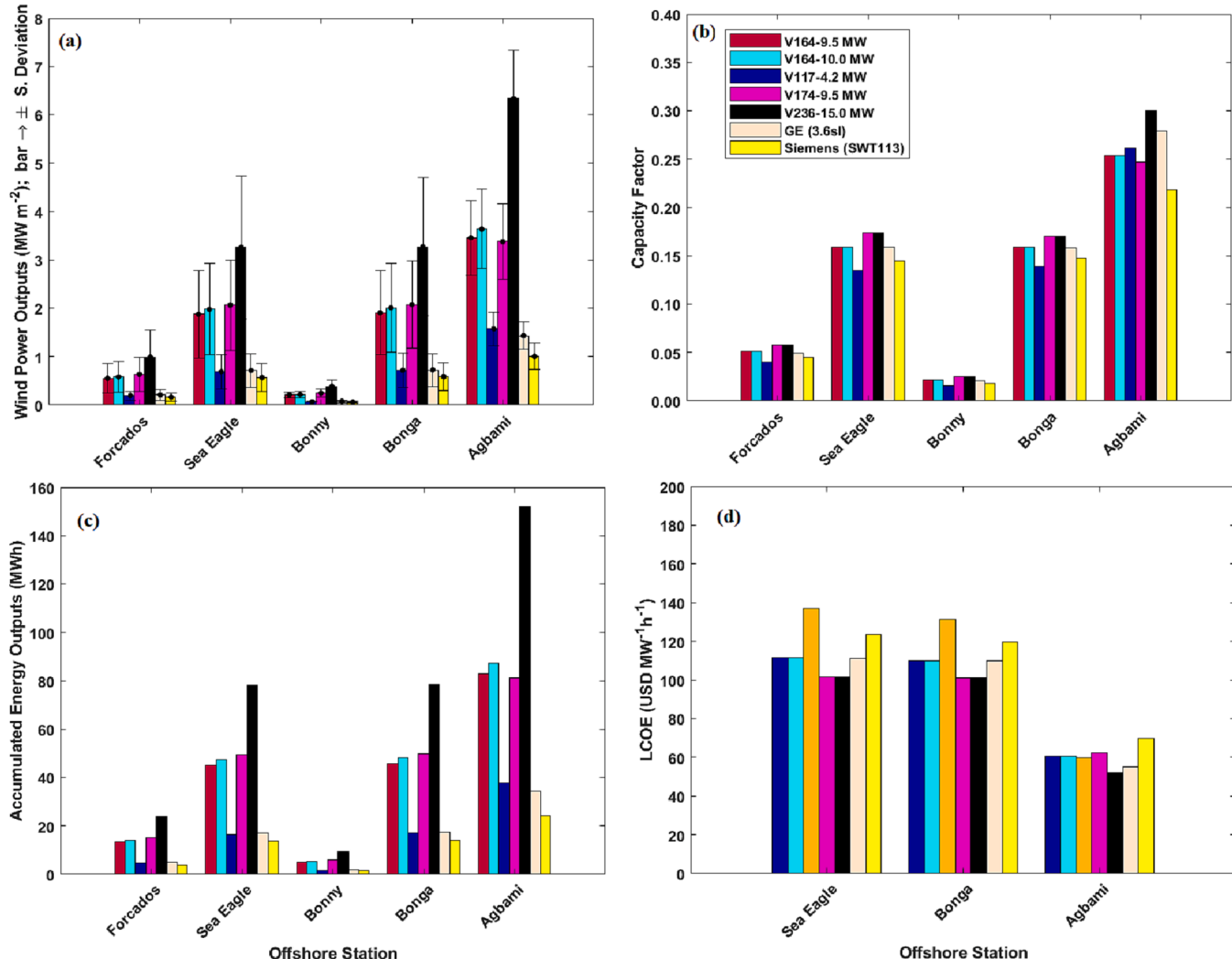


Fig. 16. Variations in annual (a) mean power outputs, (b) capacity factor, (c) accumulated mean energy outputs, and (d) Levelised Cost of Energy (LCOE) estimated for the selected turbines on the deep waters (Agbami, Bonga, and Sea Eagle) due to their moderately high-capacity factors. The coastal sites of Bonny and Forcados were excluded from LCOE estimation due to the relatively low-capacity factors with the selected offshore turbines.

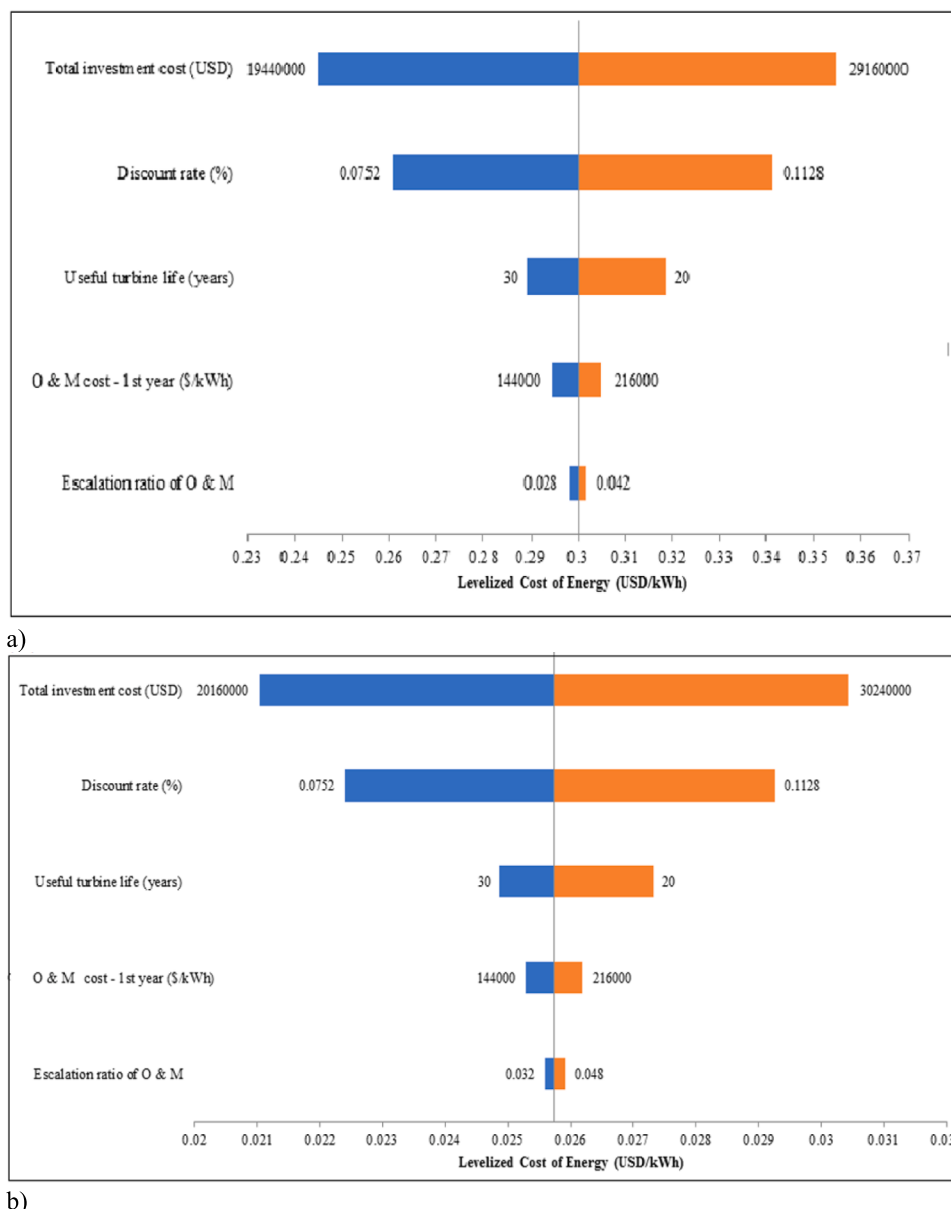


Fig. 17. Sensitivity analyses of (a) fixed-bottom substructure at Bonny site, and (b) floating substructure at Agbami offshore wind LCOE to key input parameters with V236-15 MW turbine.

5. Due to the moderately high-capacity factors observed in the deep waters of the GoG, and the improving cost competitiveness of offshore wind technology, dedicated wind farms could also be developed in these locations to run electrolyzers for producing renewable hydrogen whose versatility has the potential to contribute to the decarbonisation of several sectors, as well as providing a low-carbon source of flexibility in power systems. Renewable hydrogen could help support a clean energy transition through sector coupling (for instance, using hydrogen to reduce CO₂ emissions in transport and hard-to-abate sectors of industry such as iron, steel, and chemicals). Such dedicated wind projects would benefit from cost reductions by excluding transmission assets. Hence, the full exploitation of offshore wind resources in the GoG can effectively relieve Nigeria's power crisis, thereby meeting the country's ambitious targets of ETP set for carbon neutrality by 2060.

5. Suggestions for further study

The following are suggested for future work:

1. More input/empirical data sources on detailed system cost breakdown (such as lease price, plant commissioning, decommissioning, contingency, construction finance, insurance during construction, development, engineering management, port and staging, logistics, transportation for the fixed-bed and floating offshore plant), including industry collaboration, should be utilized to improve the accuracy of estimated LCOE in this region.
2. Studies should consider the assessment of the techno-economic viability of the selected coastal sites of Bonny and Forcados (non-windy sites) using smaller wind turbines with lower-rated power and their combination as hybrid energy systems.
3. In addition, further work should also consider using an analytical site modelling tool capable of supporting a preliminary selection of new turbine sites. This may be essential because of the increasing

competition from social, economic, and political interests for use of the seas.

CRediT authorship contribution statement

Olayinka S. Ohunakin: Conceptualization, Supervision, Data curation, Writing – original draft, Writing – review & editing, Visualization. **Olaniran J. Matthew:** Validation, Writing – review & editing. **Muyiwa S. Adaramola:** Data curation, Writing – review & editing. **Opemipo E. Atiba:** Data curation, Writing – review & editing. **Damola S. Adelekan:** Data curation, Writing – review & editing. **Oluwadamilare O. Aluko:** Writing – review & editing. **Emerald U. Henry:** Data curation, Writing – original draft. **Victor U. Ezekiel:** Writing – review & editing.

Declaration of Competing Interest

The authors declare that they have no known competing financial interests or personal relationships that could have appeared to influence the work reported in this paper.

Data availability

Data will be made available on request.

Acknowledgments

The authors wish to acknowledge the support offered by the Nigerian Upstream Petroleum Regulatory Commission (NUPRC), Abuja, and Covenant University, Ota, Ogun State, Nigeria in the actualization of this work.

References

- [1] Görüm T, Aydogan B, Ayat B. Offshore wind power potential analysis for different wind turbines in the Mediterranean Region, 1959–2020. *Energ Convers Manage* 2022;274:116470.
- [2] Chancham C, Waesak J, Gagnon Y. Offshore wind resource assessment and wind power plant optimization in the Gulf of Thailand. *Energy* 2017;139:706–31. <https://doi.org/10.1016/j.energy.2017.08.026>.
- [3] Nigeria Energy Transition Plan. <https://www.energytransition.gov.ng/#Implement> [Accessed on March 05, 2023].
- [4] Al-Hinai A, Charabi Y, Aghay Kaboli SH. Offshore wind energy resource assessment across the territory of Oman: a spatial-temporal data analysis. *Sustainability* 2021; 13:2862. <https://doi.org/10.3390/su13052862>.
- [5] Global Wind Energy Council (GWEC). Global Offshore Wind Report 2022; 29 June 2022. <https://gwec.net/gwecs-global-offshore-wind-report/> [Accessed on February 15, 2023].
- [6] Offshore Wind Market Report: 2022 Edition. US Department of Energy, Office of Energy Efficiency and Renewable Energy. https://www.energy.gov/sites/default/files/2022-08/offshore_wind_market_report_2022.pdf [Accessed on February 15, 2023].
- [7] Varela-Vazquez P, del Carmen M, Sanchez-Carreira.. Estimation of the potential effects of offshore wind on the Spanish economy. *Renew Energy* 2017;111:815–24.
- [8] Zountouridou E, Kiokes G, Chakalis S, Georgilakis P, Hatziargyriou N. Offshore floating wind parks in the deep waters of Mediterranean Sea. *Renew Sustain Energy Rev* 2015;51:433–48.
- [9] Snyder B, Kaiser M. Ecological and economic cost-benefit analysis of offshore wind energy. *Renew Energy* 2009;34:1567–78.
- [10] Sun X, Huang D, Wu G. The current state of offshore wind energy technology development. *Energy* 2012;41(1):298–312.
- [11] Carley S, Lawrence S, Brown A, Nourafshan A, Benami E. Energy-based economic development. *Renew Sustain Energy Rev* 2011;15:282–95.
- [12] Dalton GJ, Lewis T. Metrics for measuring job creation by renewable energy technologies, using Ireland as a case study. *Renew Sustain Energy Rev* 2011;15: 2123–33.
- [13] Kim J-Y, Oh K-Y, Kang K-S, Lee J-S. Site selection of offshore wind farms around the Korean Peninsula through economic evaluation. *Renew Energy* 2012;54: 189–95. <https://doi.org/10.1016/j.renene.2012.08.026>.
- [14] Nagababu G, Kachhwaha S-S, Sabsani V. Estimation of technical and economic potential of offshore wind along the coast of India. *Energy* 2017;138:79–91.
- [15] Nigeria's First Nationally Determined Contribution – 2021 Update. The Federal Government of Nigeria. Federal Ministry of Environment, Abuja. Article 4.2 of the Paris Agreement under the United Nations Framework Convention on Climate Change (UNFCCC); July 2021.
- [16] Akinsanola AA, Ogunjobi KO, Ablude AT, Sarris SC, Ladipo KO. Assessment of wind energy potential for small communities in south-south Nigeria: case study of Koltuama, Bayelsa State. *J Fund Renew Energy Appl* 2017;7(227). <https://doi.org/10.4172/20904541.1000227>.
- [17] Udo NA, Oluyeye A, Ishola KA. Investigation of wind power potential over some selected coastal cities in Nigeria. *Innovat Energy Res* 2017;6(1):1–12.
- [18] Okeniyi JO, Ohunakin OS, Okeniyi ET. Assessments of wind-energy potential in selected sites from three geopolitical zones in Nigeria: implications for renewable/sustainable rural electrification. *Scientific World J* 2015:1–13. <https://doi.org/10.1155/2015/581679>.
- [19] Ohunakin OS, Oyewola OM, Adaramola MS. Economic analysis of wind energy conversion systems using levelized cost of electricity and present value cost methods in Nigeria. *Int J Energy Environ Eng* 2012;4(2):1–8. <https://doi.org/10.1186/2251-6832-4-2>.
- [20] Ohunakin OS, Akinnawonu OO. Assessment of wind energy potential and the economics of wind power generation in Jos, Plateau State, Nigeria. *Energy Sustain Develop* 2012;16(1):78–83. <https://doi.org/10.1016/j.esd.2011.10.004>.
- [21] Ohunakin OS. Wind resources in North-East geopolitical zone, Nigeria: an assessment of the monthly and seasonal characteristics. *Renew Sustain Energy Rev* 2011;15(4):1977–87.
- [22] Ohunakin OS. Assessment of wind energy resources for electricity generation using WECS in North-Central region, Nigeria. *Renew Sustain Energy Rev* 2011;15(4): 1968–76.
- [23] Ohunakin OS, Adaramola MS, Oyewola OM. Wind energy evaluation for electricity generation using WECS in seven selected locations in Nigeria. *Appl Energy* 2011;88 (9):3197–206.
- [24] Ohunakin OS. Wind resource evaluation in six selected high-altitude locations in Nigeria. *Renew Energy* 2011;36(12):3273–81.
- [25] Adaramola MS, Oyewola OM, Ohunakin OS, Akinnawonu OO. Performance evaluation of wind turbines for energy generation in Niger Delta, Nigeria. *Sustain Energy Technol Assess* 2014;6:75–85.
- [26] Adaramola MS, Oyewola OM, Ohunakin OS, Dinrifo RR. Techno-economic evaluation of wind energy in South-West Nigeria. *Front Energy* 2012;6(4):366–78.
- [27] Olaofe ZO. Assessment of the offshore wind speed distributions at selected stations in the South-West Coast, Nigeria. *Int J Renew Energy Res* 2017;7(2).
- [28] Olaofe ZO. Review of energy systems deployment and development of offshore wind energy resource map at the coastal regions of Africa. *Energy* 2018;161: 1096–114.
- [29] Shields M, Beiter P, Kleiber W. Spatial impacts of technological innovations on the levelized cost of energy for offshore wind power plants in the United States. *Sustain Energy Technol Assess* 2021;45:101059. <https://doi.org/10.1016/j.seta.2021.101059>.
- [30] Cai Y, Breon FM. Wind power potential and intermittency issues in the context of climate change. *Energy Convers Manag* 2021;240:114276. <https://doi.org/10.1016/j.enconman.2021.114276>.
- [31] Çarpař T, Ayat B, Aydogan B. Spatio-seasonal variations in long-term trends of offshore wind speeds over the black sea; an inter-comparison of two reanalysis data. *Pure Appl Geophys* 2020;177:3013–37. <https://doi.org/10.1007/s00024-019-02361-7>.
- [32] Aydogan B. Offshore wind power atlas of the Black Sea Region. *J Renew Sustain Energy* 2017;9:013305. <https://doi.org/10.1063/1.4976968>.
- [33] Ren G, Wan J, Liu J, Yu D, Söder L. Analysis of wind power intermittency based on historical wind power data. *Energy* 2018;150:482–92. <https://doi.org/10.1016/j.energy.2018.02.142>.
- [34] Torres-Rincón S, Bastidas-Arteaga E, Sánchez-Silva M. A flexibility-based approach for the design and management of floating offshore wind farms. *Renew Energy* 2021;175:910–25.
- [35] Tummala A, Velamati RK, Sinha DK, Indraja V, Krishna VH. A review on small scale wind turbines. *Renew Sustain Energy Rev* 2016;56:1351–71. <https://doi.org/10.1016/j.rser.2015.12.027>.
- [36] Ichenni MM, El-Hajjaji A, Khamlich A. Effect of atmospheric stability on the estimation of wind power potential. *MATEC Web of Conferences* 2016;8347: 09008. <https://doi.org/10.1051/matecconf/20168309008CSNDD>.
- [37] Holtslug MC, Bierbooms WAAM, Bussel GJWV. Estimating atmospheric stability from observations and correcting wind shear models accordingly. *J Phys: Conf Ser* 2014;555:012052.
- [38] Soukissian TH, Karathanasi FE, Zaragkas DK. Exploiting offshore wind and solar resources in the Mediterranean using ERA5 reanalysis data. *Energy Convers Manag* 2021;237:114092. <https://doi.org/10.1016/j.enconman.2021.114092>.
- [39] Bhattacharya S, Pennoch S, Robertson B, Hanif S, Alam MJ, Bhatnagar D, et al. Timing value of marine renewable energy resources for potential grid applications. *Appl Energy* 2021;299:117281.
- [40] Bahrami A, Teimourian A, Okoye CO, Khosravi N. Assessing the feasibility of wind energy as a power source in Turkmenistan; a major opportunity for Central Asia's energy market. *Energy* 2019;183:415–27.
- [41] Peng X, She J, Zhang S, Tan J, Li Y. Evaluation of multi-reanalysis solar radiation products using global surface observations. *Atmos* 2019;10:42. <https://doi.org/10.3390/atmos10020042>.
- [42] Akpinar EK, Akpinar S. An assessment on seasonal analysis of wind energy characteristics and wind turbine characteristics. *Energ Convers Manage* 2005;46: 1848–67. <https://doi.org/10.1016/j.enconman.2004.08.012>.
- [43] Bosch J, Staffell I, Hawkes AD. Global levelised cost of electricity from offshore wind. *Energy* 2019;189:116357. <https://doi.org/10.1016/j.energy.2019.116357>.
- [44] Taboada JV, Diaz-Casas V, Yu X. Reliability and maintenance management analysis on offshore wind turbines (OWTs). *Energies* 2021;14:7662. <https://doi.org/10.3390/en14227662>.

- [45] Stehly T, Beiter P, Duffy P. Cost of wind energy review. National Renewable Energy Laboratory. Technical Report. NREL/TP-5000-78471; December 2020. <https://www.nrel.gov/docs/fy21osti/78471.pdf> [Accessed on February 15, 2023].
- [46] Tian Y-C, kou L, Han Y-D, Yang X, Hou T-T, Zhang W-K. Evaluation of offshore wind power in the China sea. *Energy Explor Exploit* 2021;39(5):1803–16.
- [47] Matthew OJ, Ayoola MA. Seasonality of wind speed, wind shears and precipitation over West Africa. *J Atmos Sol Terr Phys* 2020;207:105371.
- [48] Moriasi DN, Arnold JG, Van Liew MW, Bingner RL, Harmel RD, Veith TL. Model evaluation guidelines for systematic quantification of accuracy in watershed simulations. *Trans ASABE* 2007;50:885–900.
- [49] International Energy Agency (IEA). Offshore Wind Outlook 2019. https://iea.blob.core.windows.net/assets/495ab264-4ddf-4b68-b9c0-514295ff40a7/Offshore_Wind_Outlook_2019.pdf [Accessed on: March 29, 2023].
- [50] Shields M, Beiter P, Nunemaker J, Cooperman A, Duffy P. Impacts of turbine and plant upsizing on the levelized cost of energy for offshore wind. *Appl Energy* 2021; 298:117189. <https://doi.org/10.1016/j.apenergy.2021.117189>.